LEVE $\mathbb{I}$

AD A0 59074

HIGH SPEED FLOW SEPARATION
AHEAD OF FINITE SPAN STEPS

Louis G. Kaufman II, LTC, USAFR
Robert D.Kirchner, CAPT, USAFR
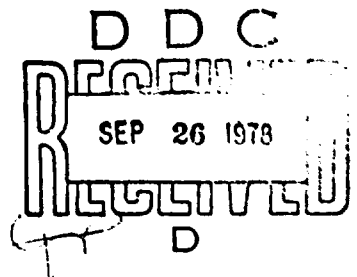AERONAUTICAL SYSTEMS DIVISION (ASD)

HIGH SPEED AERO PERFORMANCE BRANCH (FXG)
AEROMECHANICS DIVISION (FX)

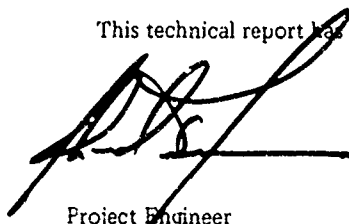DDC FILE COPY

DDC
SEP 26 1978
RECEIVED
D

78 08 16 015

Best Available Copy

NOTICE

When Government drawings, specifications, or other data are used for any purpose other than in connection with a a definitely related Government procurement operation, the United States Government thereby incurs no responsibility nor any obligation whatsoever, and the fact that the government may have formulated, furnished, or in any way supplied the said drawings, specifications, or other data, is not to be regarded by implication or otherwise as in any manner licensing the holder or any other person or corporation, or conveying any rights or permission to manufacture, use, or sell any patented invention that may in any way be related thereto.
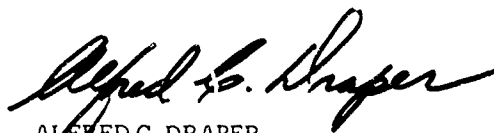
This report has been reviewed by the Office of Information (OI) and is releasable to the National Technical Information Service (NTIS). At NTIS, it will be available to the general public, including foreign nations.

This technical report has been reviewed and is approved for publication.

Project Engineer

FOR THE COMMANDER

ALFRED C. DRAPER
Asst. For Research and Technology
Flight Mechanics Division

REPORT DOCUMENTATION PAGE		READ INSTRUCTIONS BEFORE COMPLETING FORM
1 REPORT NUMBER AFFDL-TR-78-30	2 GOVT ACCESSION NO	3 RECIPIENT'S CATALOG NUMBER
4 TITLE (and Subtitle) HIGH SPEED FLOW SEPARATION AHEAD OF FINITE SPAN STEPS		5 TYPE OF REPORT & PERIOD COVERED Technical - Final July 1974 - July 1977
		6 PERFORMING ORG REPORT NUMBER
7 AUTHOR(s) Louis G. Kaufman, II LTC, USAFR Robert D. Kirchner CAPT, USAFR		8 CONTRACT OR GRANT NUMBER(s) Internal
9 PERFORMING ORGANIZATION NAME AND ADDRESS Air Force Flight Dynamics Laboratory (FXG) Air Force Systems Command Wright-Patterson AF Base, Ohio 45433		10 PROGRAM ELEMENT PROJECT TASK AREA & WORK UNIT NUMBERS ASD Reserve Officer's Project 75-105
11 CONTROLLING OFFICE NAME AND ADDRESS Aeronautical Systems Division Air Force Systems Command Wright-Patterson AF Base, Ohio 45433		12 REPORT DATE April 1978
		13 NUMBER OF PAGES 73
14 MONITORING AGENCY NAME & ADDRESS(if different from Controlling Office)		15 SECURITY CLASS (of this report) UNCLASSIFIED
		15a DECLASSIFICATION DOWNGRADING SCHEDULE

16 DISTRIBUTION STATEMENT (of this Report)

Approved for public release: distribution unlimited.

17 DISTRIBUTION STATEMENT (of the abstract entered in Block 20, if different from Report)

Final rept. Jul 74 - Jul 77,

18 SUPPLEMENTARY NOTES

19 KEY WORDS (Continue on reverse side if necessary and identify by block number)

Separation, Steps, Turbulent Boundary Layer, Supersonic, Hypersonic, Heat Transfer, Flat Plate

20 ABSTRACT (Continue on reverse side if necessary and identify by block number)

Detailed surface heat transfer data, oil flow, and schlieren photographs are presented for high speed flow separation ahead of finite span, forward facing steps on flat plates. Step spans were varied from three to ten times as large as the step height, and the step heights are three to four times larger than the undisturbed turbulent boundary layer thickness. Reynolds numbers, based on plate length, were approximately 15 million for both Mach 4.75

DD $_{1 \text{ JAN } 73}^{\text{FORM}}$ 1473 EDITION OF 1 NOV 65 IS OBSOLETE
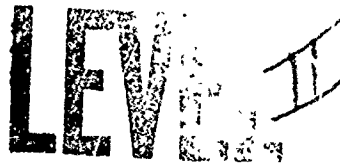
012 070

and Mach 5.04 local undisturbed flows over the flat plate surface. For these test conditions, the maximum extent of separation ahead of the step is approximately 4.4 times as large as the step height independent of step span, and peak heating rates were measured that are more than six to eight times larger than the undisturbed flow heating rates. Peak heating on the plate surface occurs slightly upstream and approximately 1/2 step height inboard of the outboard sides of the steps, the increase in peak heat transfer coefficients over the undisturbed flow values decreases with increasing step span. In addition to presenting the detailed surface heat transfer data, a plausible theoretical analysis is presented for calculating the region of turbulent boundary layer separation ahead of these finite span steps.

LEVEL II

FOREWORD

Results of the experimental and analytical investigation
described herein were obtained under Air Force Task 240407
"Aeroperformance and Aeroheating Technology." The Project Monitor
was Richard Neumann of the High Speed Aero Performance Branch
(FXG), Aeromechanics Division, Air Force Flight Dynamics
Laboratory (AFFDL), Wright-Patterson Air Force Base, Ohio. Mr.
Neumann conceived the research program and directed the work.
The authors thank him for his guidance and help throughout the
program.

The authors also wish to thank James R. Hayes (AFFDL/FXG)
for his assistance in supplying details of the experimental
apparatus used and for the data, which were obtained during
an earlier portion of the program. The current work comprised
reducing, analyzing, and presenting the experimental results.
This later portion of the program was accomplished by AF Reserve
Officers assigned to the Aeronautical Systems Division (ASD)
of the Air Force Systems Command (AFSC) under ASD Reserve Project
75-105. LTC Kaufman is a Senior Staff Scientist for Grumman
Aerospace Corporation, Bethpage, N.Y., and CAPT Kirchner is a
Physical Science Instructor, Chesterfield County, Virginia Public
School System. The authors express their gratitude to their
fellow ASD Reserve Officers, Myron D. Goldman, MAJ, USAFR and
Harold O. Jensen, CAPT, USAFR, for their engineering and
drafting assistance in preparing this report.

TABLE OF CONTENTS

LIST OF ILLUSTRATIONS

LIST OF ILLUSTRATIONS (cont'd)

LIST OF ILLUSTRATIONS (cont'd)

LIST OF SYMBOLS

b   step span

c   specific heat of model wall material

h   aerodynamic heat transfer coefficient

ℓ extent of separated flow region upstream of step face

m   source strength

M   Mach number

p   pressure

$\dot{q}$ aerodynamic heat transfer rate

Re   Reynolds number

t   time

T   temperature

U   stream flow velocity

w   density of model wall material

x,y,z   orthogonal coordinate system with origin at step face
             (see Fig. 2)

α angle of attack of flat plate surface

γ ratio of specific heats of air (taken as 1.4 herein)

δ boundary layer thickness

ϵ flow deflection angle at separation

τ shock wave angle

ξ dummy variable of integration, Eq. (11)

τ thickness of wall at thermocouple location

ψ stream function

Subscripts

o   stagnation conditions

1   flow conditions over flat plate surface

∞ tunnel free stream flow conditions

awT   adiabatic wall conditions for turbulent boundary layer

sep   conditions at the location of flow separation

und   local undisturbed flow conditions (values on the flat plate surface when no step is attached)

w   wall conditions

SECTION I

INTRODUCTION

Flow separation can substantially alter the anticipated loads and heating rates on high speed aircraft surfaces, and can compromise an aircraft design. The importance of this problem is well recognized and has prompted many investigations of shock-induced separated flows (e.g., Refs. 1-40). Although important to practical aircraft design, three dimensional separated flow problems are quite complex and are not amenable to theoretical solutions at present. The subject work was undertaken to obtain a better understanding of some important three dimensional flow effects for a relatively basic geometry: flow separation ahead of finite span, forward facing steps.

The character of the boundary layer and the ratio of the step height to the undisturbed boundary layer thickness strongly affect the extent of flow separation ahead of steps. These effects have been investigated for high aspect ratio, essentially "two dimensional" steps (Refs. 6, 17, 35, 36, and 38). The subject work complements these existing separated flow investigations and includes finite span effects.

Steps of various spans were mounted on an existing large flat plate model. Flow conditions, step height, model size, and attitude were chosen to ensure turbulent boundary layer flow on the flat plate surface prior to the onset of separation. All steps had the same height, which was chosen to be several times larger than the undisturbed boundary layer thickness. Dense arrays of surface aerodynamic heat transfer rate data were obtained, as well as planform oil film flow and profile schlieren photographs. The data were analyzed, compared with some analytical results, and are presented herein.

1

SECTION II

EXPERIMENTAL APPARATUS, FLOW CONDITIONS, AND TEST PROCEDURE

1 Model

Planform and profile views of the flat plate forward facing step model are sketched in Figure 1. An existing FDL flat plate model, which had been used in an earlier experimental program (Ref. 23), was modified for the present experiments. The flat plate portion of the model has a 24-inch span and a 26.5-inch chord. The face of the model forms an angle of 30.5° with the flat plate surface, and the leading edge is ground sharp.

A 10-inch square portion of the flat plate surface, centered mid-span and terminating at the plate trailing edge, is instrumented with thermocouples. Thermocouples are spot welded to the inner surface of thin wall portions of the insert to enable one to obtain aerodynamic heating rates using the thin wall transient temperature technique (Ref. 23). The thermocouples are spaced at 0.50-inch intervals along three chordwise lines, and at 0.25-inch intervals along two chordwise lines. The five chordwise lines are two inches apart.

Forward facing steps of 3-, 5-, 7-, and 10-inch spans were fabricated. The steps have 2-inch chords, heights of 1-inch, and are attachable at different locations near the trailing edge of the flat plate surface. The steps can be shifted forward 0.125-inch from the furthest aft location, and can be shifted spanwise in 0.5-inch intervals. Shifting the step location between tunnel runs permits obtaining thermocouple data at 0.125-inch intervals along chordwise lines 0.5-inch apart. The steps are sealed and insulated from the flat plate surface by a layer of teflon. A step oriented coordinate system

2

is shown in Figure 2. The origin is centered at the step mid-span where the forward face of the step meets the flat plate surface.

2 Wind Tunnel

The subject experiments were conducted in the von Karman Facility Tunnel B at Arnold Engineering Development Center (AEDC). This is a continuous flow, closed-circuit, variable density wind tunnel. It has replaceable, axisymmetric, contoured nozzles to provide either nominally Mach 6 or Mach 8 free stream flows in the 50-inch diameter test section (Ref. 41). A model injection system is located in a cabin directly beneath the test section; the model may be injected into the tunnel flow and then ejected without interrupting the tunnel flow. A front view photograph of the model mounted on the injection system in the cabin beneath the test section is shown in Figure 3. In this photograph, the 10-inch span forward facing step is attached to the model.

3 Flow Conditions

In order to provide data for turbulent boundary layer separation, tunnel stagnation pressure (p_o) and temperature (T_o) values were chosen that result in a relatively high unit Reynolds number (Re_∞/ft) in the nominal Mach 6 free stream flow. However, when the plate was aligned with the free stream flow, a turbulent boundary layer was not fully developed on the plate surface until further downstream than desired. Therefore, the model was pitched nose downward (flat plate surface in compression), in order to increase the local flow unit Reynolds number and cause boundary layer transition to occur further forward. Two angles of attack were chosen: $\alpha = -6.8^\circ$ and $\alpha = -9.0^\circ$.

The local Mach numbers (M_1) of the resulting flows over the flat plate surface were: $M_1 = 5.04$ and $M_1 = 4.75$.

Tunnel flow stagnation conditions, free stream flow static conditions, and local flow conditions over the flat plate surface are listed in Table I. Free stream conditions are denoted by subscript ∞, local flow conditions over the pitched flat plate surface are indicated by subscript 1. The adiabatic wall temperature for turbulent boundary layer flow over the flat plate surface (T_{awT}) is computed using a turbulent recovery factor of 0.89

$$\frac{T_{awT}}{T_o} = \frac{1 + 0.178 \, M^2}{1 + 0.2 \, M^2} \tag{1}$$

TABLE 1 FLOW CONDITIONS

		α (deg)	-6.8	-9.0
p_o (psia)	284	p_{o1} (psia)	262	241
T_o ($^\circ$R)	850	T_{o1} ($^\circ$R)	850	850
M_∞	5.95	M_1	5.04	4.75
$Re_\infty/10^6$ ft	5.33	$Re_1/10^6$ ft	7.37	7.78
p_∞ (psia)	0.189	p_1 (psia)	0.473	0.613
T_∞ ($^\circ$R)	105	T_1 ($^\circ$R)	140	154
T_{awT} ($^\circ$R)	768	T_{awT} ($^\circ$R)	772	773

4

4 Data and Test Procedure

Data were obtained on five basic model configurations (flat plate alone or with any one of four forward facing steps of different spans), at two model angles of attack (-6.8 and -9.0°). Aerodynamic heating rate distributions on the flat plate surface and profile schlieren flow photographs were obtained for all configurations at both angles of attack. As indicated in Table II, planform oil film flow motion pictures were obtained when the steps were attached to the flat plate model at $\alpha = -6.8°$ ($M_1 = 5.04$), and when the 10-inch span step was attached to the flat plate model at $\alpha = -9.0°$ ($M_1 = 4.75$). Several tunnel runs were duplicated to ascertain the repeatability of the data.

TABLE 2 DATA

M_1	Step Span (Inches)				
	0	3	5	7	10
5.04	h sch	h oil sch	h oil sch	h oil sch	h oil sch
4.75	h sch	h sch	h sch	h sch	h oil sch

h: heat transfer coefficient distribution
oil: oil film flow motion pictures
sch: schlieren flow photographs

Aerodynamic heat transfer rates, $\dot{q}$, are proportional to the rate at which the surface temperature rises on a thin wall model (Refs. 9, 16, and 23)

$$\dot{q} = w\tau c(dT_w/dt) \tag{2}$$

where w is the density of the model wall material, τ is the thickness of the wall at the thermocouple location, c is the specific heat of the model wall material, T_w is the surface wall temperature, and t is time. The aerodynamic heat transfer coefficient used herein is

$$h = \dot{q}/(T_{awT} - T_w) \qquad (3)$$

To obtain the heating rates, the model is cooled to essentially room temperature (approximately $535°R$) and then quickly injected* into the tunnel flow. Temperatures measured by each thermocouple are recorded at the rate of 20/sec for several seconds. The model is then ejected from the tunnel flow. Linear portions of curve fits to the temperature time histories are used to calculate the values of (dT_w/dt). Errors due to conduction, radiation, and nonuniform flow heating† are minimized by using the linear portions of the temperature-time curves; the errors are negligible for the subject experiments (Refs. 9, 16, and 23).

Dense aerodynamic heating rate distributions were obtained by shifting the step location from run to run and injecting the model again into the same tunnel flow. Thus, up to eight runs were used to record temperature data for one step configuration. This effectively increases the thermocouple location density eightfold. Profile schlieren flow photographs were taken while the temperature data were being measured and recorded.

Additional tunnel runs were required to obtain planform oil film flow motion pictures. The flat plate surface was coated

---
† Full injection from cabin to tunnel centerline takes approximately two seconds. The model passes through the tunnel wall free shear layer and experiences nonuniform flow heating for less than one second.

with a mixture of titanium dioxide and silicone oil and the
model injected into the tunnel flow. High resolution motion
pictures of the surface oil film flow were obtained using
70 mm film and a framing rate of 10/sec.

SECTION III

EXPERIMENTAL RESULTS

Data are presented first for flows over the flat plate model
with no step attached. Streamwise distributions of the aerody-
namic heat transfer coefficients on the flat plate surface at
$\alpha = -6.8^\circ$ ($M_1 = 5.04$) and at $\alpha = -9.0^\circ$ ($M_1 = 4.75$), referred
to as $h_{und}(x)$, are used to nondimensionalize the heat transfer
coefficients measured on the plate surface when various span
steps are attached to the model.

1 Flows Over Flat Plate Without Steps

The coordinate system origin, when there is no step, is
taken along the flat plate surface centerline, 23.75 inches
downstream of the plate leading edge (cf. Figures 1 and 2).
Boundary layer thicknesses at $x = 0$, scaled from profile
schlieren photographs (Figure 4), are approximately: 0.29-inch
for $\alpha = -6.8^\circ$ and 0.27-inch for $\alpha = -9.0^\circ$. These values
agree closely with those calculated using the Anderson and Lewis
(Ref. 42) method. (The local flow running length Reynolds num-
bers at $x = 0$ are approximately 14.6 million for $\alpha = -6.8^\circ$
and 15.4 million for $\alpha = -9.0^\circ$.)

Aerodynamic heat transfer coefficients for the flows over
the flat plate surface with no step attached are indicated in
Figures 5 and 6 for $M_1 = 5.04$ and 4.75. Measured heat trans-
fer coefficient values are indicated by symbols along the five
streamwise lines of thermocouples for both angles of attack
(Figures 5 and 6). The measured heating rates agree fairly well
with those calculated using the Anderson and Lewis method
(Ref. 42), and exhibit no consistent anomaly. The solid lines

8

that pass through the data points in Figures 5 and 6 were taken
to be representative of the heat transfer rate coefficient dis-
tributions for the local flat plate flows undisturbed by steps.
These $h_{und}(x)$ distributions were used to nondimensionalize the
heat transfer rate coefficient distributions measured at all
spanwise stations. The distributions are given by

$$h_{und} = (4.45 - 0.415 \ x)10^{-3} \qquad for \qquad M_1 = 5.04$$

and by $\qquad\qquad\qquad\qquad\qquad\qquad\qquad\qquad\qquad\qquad\qquad\qquad\qquad$ (4)

$$h_{und} = (5.40 - 0.0508 \ x)10^{-3} \qquad for \qquad M_1 = 4.75$$

Nondimensionalizing the data in coefficient form, and using con-
sistent values for the local undisturbed flow heat transfer co-
efficient distributions, avoids compounding errors caused by
minor variation in thermocouple readings or tunnel flow condi-
tions from run to run.

Heat transfer coefficients for the undisturbed local $M_1 =$
5.04 flow over the flat plate surface, nondimensionalized by
values calculated using Eq. (4), are indicated in the "carpet"
plot shown in Figure 7. In this figure, the ratio of the heat
transfer coefficients is plotted at the corresponding thermo-
couple locations on the flat plate. The repeatability of the
heat transfer coefficient ratios, ascertained by comparing values
from repeat tunnel runs, is approximately 3 percent (standard
deviation = 2.5 percent). A similar plot of heat transfer rate
coefficient ratios, for the $M_1 = 4.75$ local undisturbed flow
over the flat plate surface, is shown in Figure 8.

2   M_1 = 5.04 Flows Over Flat Plate - Step Models

Photographic and heat transfer rate data were obtained for
M_1 = 5.04   (= -6.8°)   for steps having spans of   3, 5, 7,   and
10-inches.   A profile schlieren flow photograph or the 3-inch
span step is shown in Figure 9.   Streamwise distributions of
heating rate coefficients on the flat plate surface ahead of the
3-inch   step, nondimensionalized using the undisturbed flow heat-
ing rate coefficient distribution Eq. (4) , are plotted in
Figure 10 on the same page.   Curves are faired through data ob-
tained along the centerline and along lines   1-inch   outboard
(on either side) of the centerline.   The highest heating occurs
along the outboard lines, approximately   0.2-inch   upstream of
the step face.

A frame from the planform oil film flow motion picture shows
an oil accumulation line ahead of the   3-inch   step indicative of
flow separation (Figure 11).   This line is superimposed on the
carpet plot of the measured heat transfer coefficient ratios
shown in Figure 12.   The oil accumulation line passes through the
region where there is an initial rise in the heat transfer coef-
ficient ratios.   Contours of constant values of (h/h_{und}) are
drawn in Figure 13.   Alternate contours are dashed simply as an
aid in distinguishing them.   The highest heat transfer coeffi-
cient ratio contour $(h/h_{und}$ = 8)$,   occurs just upstream of the
step face between   0.5   and   1.0-inch   outboard from the step
centerline.

Profile schlieren photograph and streamwise distributions of
heat transfer coefficient ratios ahead of the   5-inch   span step
are shown on the same page in Figures 14 and 15.   The oil film
flow photograph, carpet plots of heat transfer coefficient ratios,

and contours of constant (h/h_{und}) values are shown in
Figures 16-18. Similar data for the 7-inch span step are
shown in Figures 19-23. Data for the 10-inch span steps are
given in Figures 24-28. In all cases, measured peak heating
rates occur approximately 0.2-inch ahead of the step face and
approximately 0.5-inch inboard of the outboard edge of the
step.

3   M_1 = 4.75 Flows Over Flat Plate - Step Models

A profile schlieren photograph for M_1 = 4.75 flow (α =
-9.0°) over the flat plate with a 3-inch span step is shown
in Figure 29. Streamwise heat transfer coefficient ratios on
the plate surface ahead of the 3-inch span step are plotted
in Figure 30 on the same page. Carpet plots of the heat trans-
fer coefficient ratios and contours of constant values of
(h/h_{und}) are shown in Figures 31 and 32. Similar data for the
5- and 7-inch span steps are presented in Figures 33-40.
Planform oil film flow photographs were not obtained for these
configurations (cf. Table II).

A profile schlieren photograph and streamwise distributions
of heat transfer coefficient ratios for the 10-inch span step
on the flat plate at α = -9.0° are shown in Figures 41 and 42.
A planform oil film flow photograph for this configuration is
shown in Figure 43. The oil accumulation line apparent in
Figure 43 is superimposed on the carpet plot of the heat trans-
fer coefficient ratios given in Figure 44. Lines of constant
(h/h_{und}) contours are shown in Figure 45. Similarly to the
model configurations pitched at α = -6.8°, the highest heating
rates on the plate surface pitched at α = -9.0° occur approxi-
imately 0.2 inch upstream of the step face and 0.5-inch in-
board of the outboard edge of the step.

As noted earlier, heat transfer data were obtained during several repeat tunnel runs. For the 10-inch step on the flat plate at $\alpha = -9.0°$, the average deviation in the heat transfer coefficient ratio value is 0.025, the standard deviation is 0.037.

4 Discussion of Experimental Results

The apparent boundary layer thickness immediately upstream of flow separation δ_{sep}, and the apparent length of separated flow upstream of the step face, ℓ_{sep}, scaled from the profile schlieren flow photographs, are listed in Table III. For these experiments, the boundary layer thickness and maximum extent of separation are independent of the step span. The apparent boundary layer thickness just upstream of separation is slightly less for $\alpha = -9.0$ than for $\alpha = -6.8°$. The extent of separation, apparent in the profile schlieren flow photographs, is approximately the same for both angles of attack. The separation lengths listed in the table match closely the distances from the step faces to the oil accumulation lines scaled from the planform oil film flow photographs. Apparent in the planform oil film flow photographs, and indicated in the heat transfer coefficient ratio carpet plots, the streamwise extent of separation generally

TABLE 3   APPARENT BOUNDARY LAYER THICKNESS AT SEPARATION
AND EXTENT OF SEPARATED FLOW REGION

M_1	δ_{sep} (in.)	ℓ_{sep} (in.)
5.04	0.26	4.35 ± 0.15
4.75	0.24	4.35 ± 0.15

is greatest near the centerline and diminishes outboard. The streamwise thickness of the oil accumulation line is comparable to or smaller than the local boundary layer thickness.

For all test cases, the highest heating on the plate occurs approximately 0.2-inch forward of the step face and 0.5-inch inboard from the outboard edge of the step. The peak heat transfer coefficient ratio values are largest for the smallest step spans, and decrease monotonically with increasing step span for both angles of attack. The peak heat transfer coefficients exceed 6 to 8 times those for the local undisturbed flows, depending on step span. Average values of the heat transfer coefficients in the separated flow region are approximately 2.5 times as large as those for the undisturbed flows over the flat plate surfaces.

SECTION IV

ANALYTIC METHOD

An analytic method was devised for calculating the extent and shape of the separated flow region upstream of finite span steps. The method gives results in good agreement with the subject data but, because of several assumptions, must be considered empirical until better rationale are developed for the derivation of the method. Its application to different flow conditions is not warranted until more extensive empirical verification is provided or until a rational proof of the validity of the derivation of the method is established.

The method for estimating the extent of separation is based on the observation that the difference between the shock wave angle and the effective flow deflection angle at the onset of separation is a minimum when turbulent boundary layer separation occurs ahead of a forward facing step. The shape of the separation line on the plate surface follows from the assumption that hypersonic, turbulent boundary layer separation is driven by flow conditions in the outer, inviscid flow and that the subsonic separated flow region can be approximated by a linear source distribution with its strength dependent upon the extent of separation along the centerline.

1 Extent of Separation

The extent of separation along the centerline ahead of a forward facing step depends on the step height and the effective angle of the streamline dividing the separated flow from the outer, inviscid flow. The oblique shock wave, θ, and inviscid flow deflection angle, ϵ, are related by (Refs. 43 and 44)

14

$$\tan(\theta - \epsilon) = \frac{(\gamma-1)M_1^2 \sin^2\theta + 2}{(\gamma+1)M_1^2 \sin^2\theta} \tan\theta \tag{5}$$

Rewriting the equation as

$$\tan(\theta - \epsilon) = \frac{\gamma-1}{\gamma+1} \tan\theta + \frac{4}{(\gamma+1)M_1^2 \sin 2\theta} \tag{6}$$

and setting the partial derivative of $\tan(\theta - \epsilon)$ with respect to θ equal to zero yields

$$\frac{\gamma-1}{8} M_1^2 = \frac{\cos^2\theta \cos 2\theta}{\sin^2 2\theta} \tag{7}$$

which may be simplified for computational purposes to

$$\frac{\gamma-1}{2} M_1^2 = \frac{1 - 2\sin^2\theta}{\sin^2\theta} \tag{8}$$

For the subject experiments, flow separation occurs where $[\tan(\theta - \epsilon)]$ is a minimum. Equation (8) may be used to relate the upstream Mach number and shock wave angle at the onset of turbulent boundary layer separation ahead of the steps tested in this program. (In these epxeriments the step height is larger than the boundary layer thickness, but not so large that a strong detached shock wave forms ahead of the step.)

Once θ is determined for M_1, the flow deflection angle (ϵ) can be determined using other oblique shock relations, such as (Refs. 43 and 44)

$$\tan\epsilon = 2 \frac{M_1^2 \sin^2\theta - 1}{M_1^2(\gamma + \cos 2\theta) + 2} \cot\theta \tag{9}$$

15

Assuming that the dividing streamline for the separated flow re-attaches essentially at the top of the forward face of the step

$$\ell_{sep} = \frac{h}{\tan \epsilon}$$

therefore

$$\ell_{sep} = \frac{M_1^2 (\gamma + \cos 2\epsilon) + 2}{2(M_1^2 \sin^2 \epsilon - 1)} h \tan \epsilon \qquad (10)$$

Equations (8) and (10) may be used to calculate the extent of separation, ℓ_{sep}, upstream of forward facing steps.

2 Planform Shape of Separated Flow Region

The region of separated flow ahead of finite span steps on a plate surface is calculated assuming that a line source distribution exists along the step, perpendicular to the flow. The line source distribution is expressed by the relationship

$$\psi = \frac{m}{2\pi b} \int_{-b/2}^{b/2} \tan^{-1} \left(\frac{y - \xi}{x}\right) d\xi \qquad (11)$$

where b is the step span and m is the source strength. Integrating this expression and superimposing it upon a uniform free stream function gives

$$\psi = U_1 y + \frac{m}{2\pi b} \left\{ (y+\frac{b}{2}) \tan^{-1}\left(\frac{y+\frac{b}{2}}{x}\right) - (y-\frac{b}{2}) \tan^{-1}\left(\frac{y-\frac{b}{2}}{x}\right) \right.$$

$$\left. + \frac{x}{2} \ln \left[\frac{x^2 + (y-\frac{b}{2})^2}{x^2 + (y+\frac{b}{2})^2}\right] \right\} \qquad (12)$$

16

The strength of the source (m), established from bound ry conditions, is a function of the separation length ℓ_{sep} given by Eq. (10)]

$$m = \pi b U_1 \left[\tan^{-1} \left(\frac{b/2}{\ell_{sep}} \right) \right]^{-1} \tag{13}$$

Using zero as the constant value of the stream function ψ along the separation line and the value for the source strength given by Eq. (13), the separation line shape can be calculated from

$$0 = 2y \tan^{-1} \left(\frac{b/2}{\ell_{sep}} \right) + \left(y + \frac{b}{2} \right) \tan^{-1} \left(\frac{y + \frac{b}{2}}{x} \right) \tag{14}$$

$$- \left(y - \frac{b}{2} \right) \tan^{-1} \left(\frac{y - \frac{b}{2}}{x} \right) + \frac{x}{2} \ell n \left[\frac{x^2 + \left(y - \frac{b}{2} \right)^2}{x^2 + \left(y + \frac{b}{2} \right)^2} \right]$$

Sample plots of separation lines calculated in this manner are compared with the observed oil accumulation line shapes in Figures 46-49 for $M_1 = 5.04$. For these cases, there is generally good agreement between the experimental and analytical separation lines calculated as described above.

17

SECTION V

CONCLUSIONS

These conclusions pertain to turbulent boundary layer separation ahead of finite span, forward facing steps on flat plate surfaces. The step spans tested were three to ten times as large as the step height, and the step height is three or four times as large as the undisturbed boundary layer thickness. The results discussed were obtained for local undisturbed flow Mach numbers of 4.75 and 5.04 and Reynolds numbers of approximately 15 million, based on plate length upstream of the steps.

The maximum extent of flow separation upstream of the steps varies approximately from 4.2 to 4.5 times as large as the step height, independent of the step spans tested. The average heat transfer to the surface in the separated flow region is approximately 2.5 times larger than for the undisturbed flows over the flat plate surfaces. Local regions of peak heating occur slightly upstream of the step face at locations approximately $\frac{1}{2}$ step height inboard from the side edges of the steps. The amplification of the heat transfer coefficients in these local regions of peak heating approaches nine for the three-inch span steps. The peak heating amplification factor diminishes somewhat with increasing step span. However, the location of peak heating to the plate surface, with respect to the face and side edges of the steps, does not vary with step span. Results of derived analytical expressions for the maximum extent of separation and for the shape of the separation line on the plate surface agree with the experimental results for these test conditions.
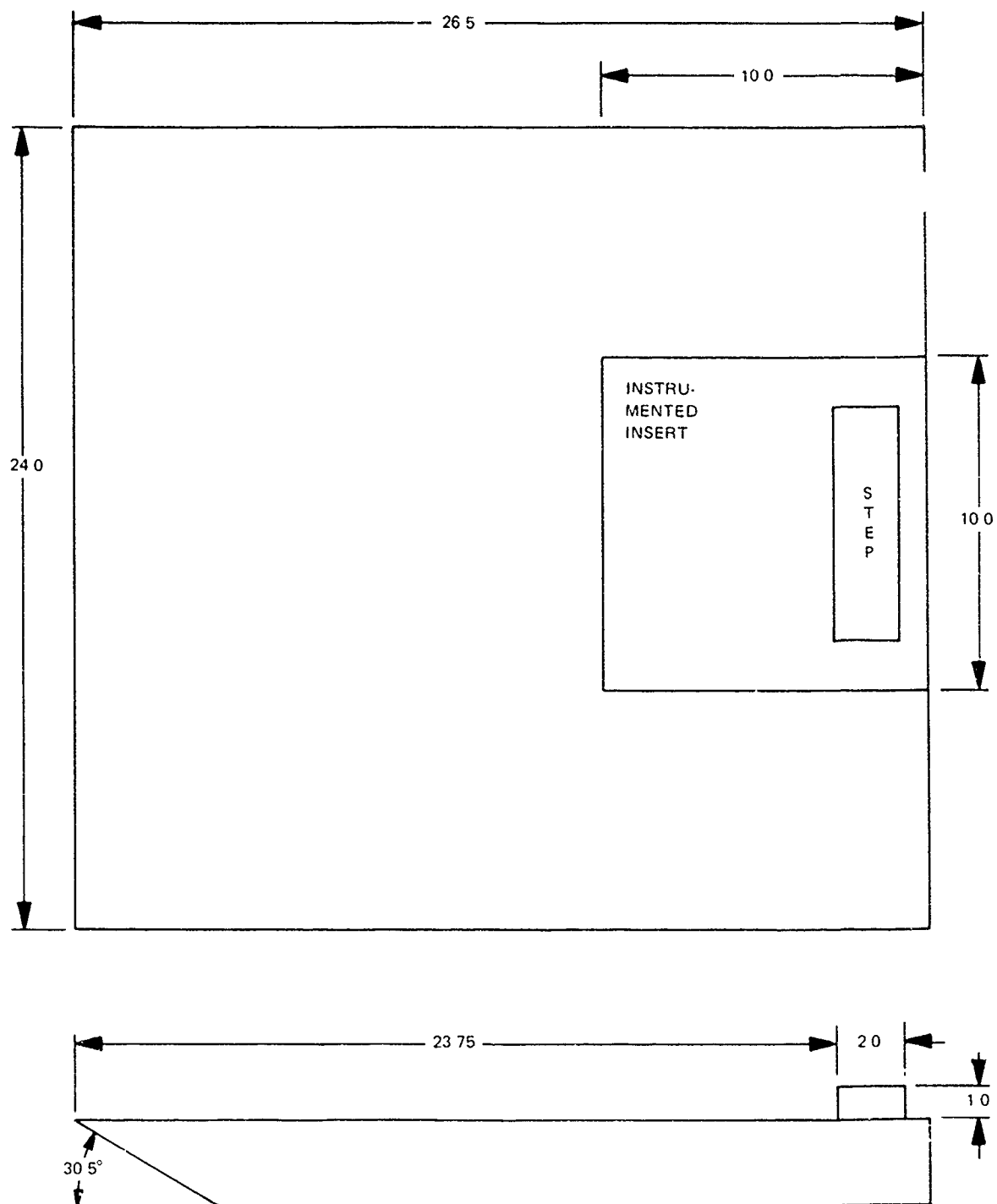
NOTE ALL LINEAR DIMENSIONS IN INCHES

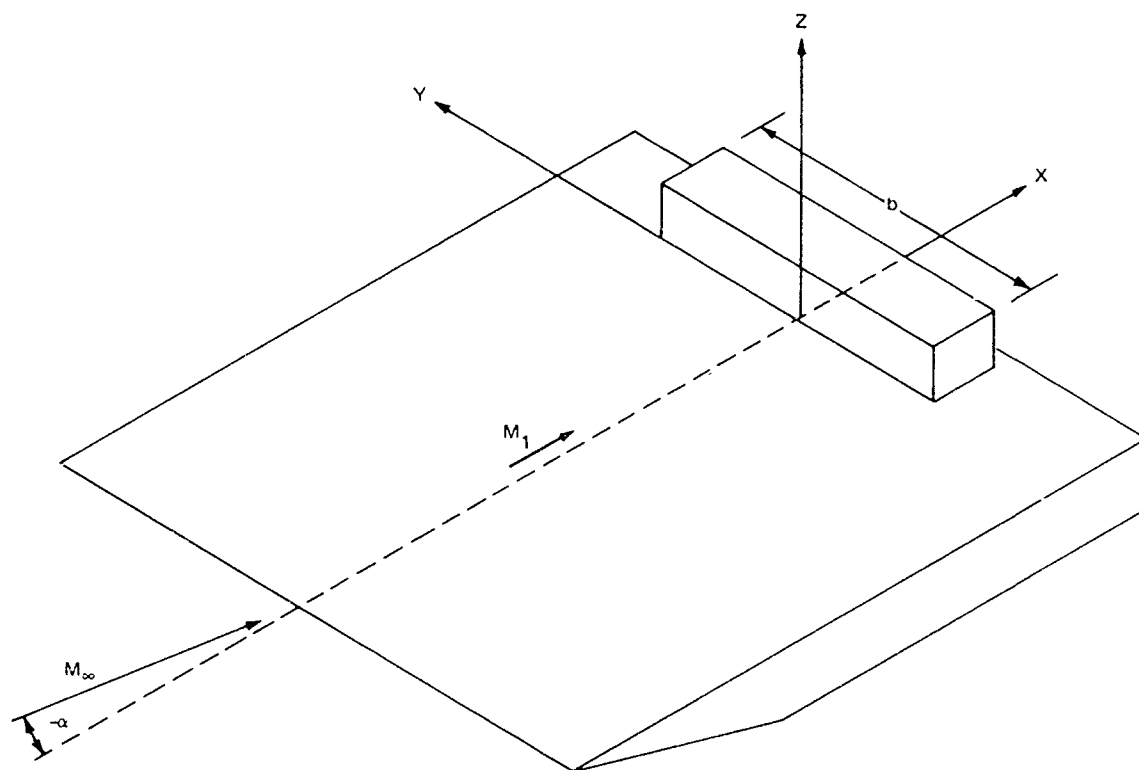Figure 1 Planform and Profile Sketches of Model with Step in Furthest Aft Location
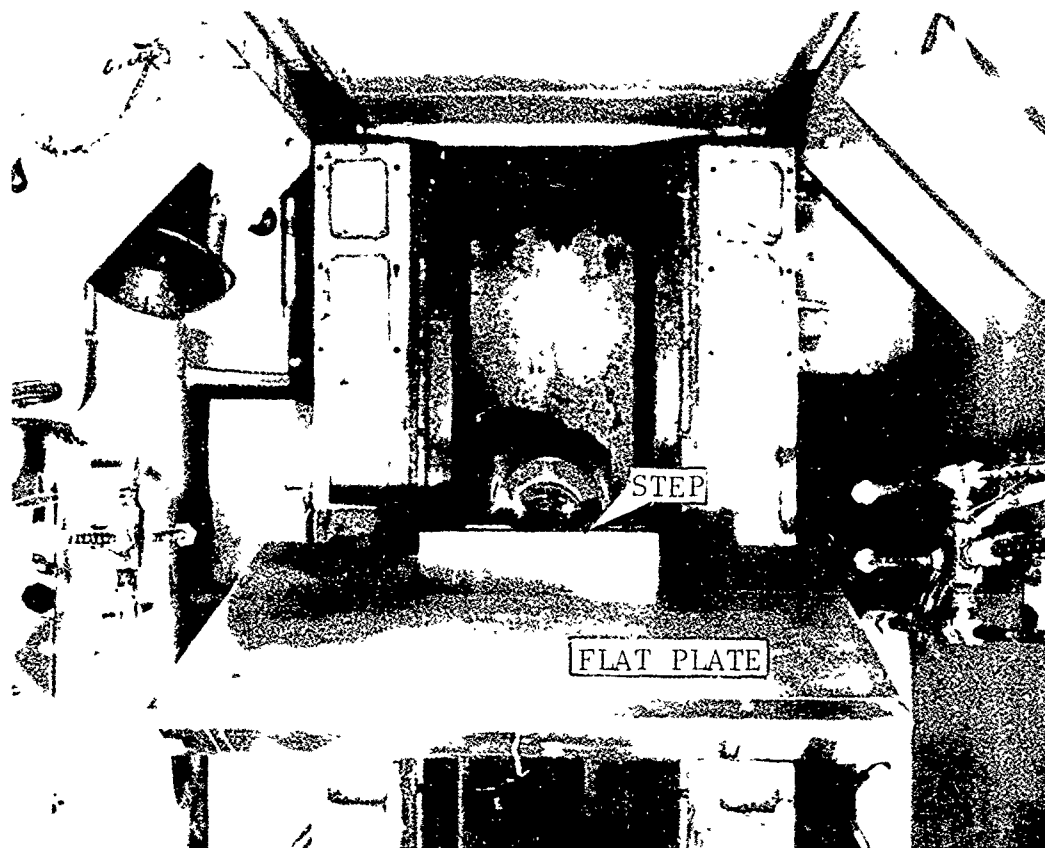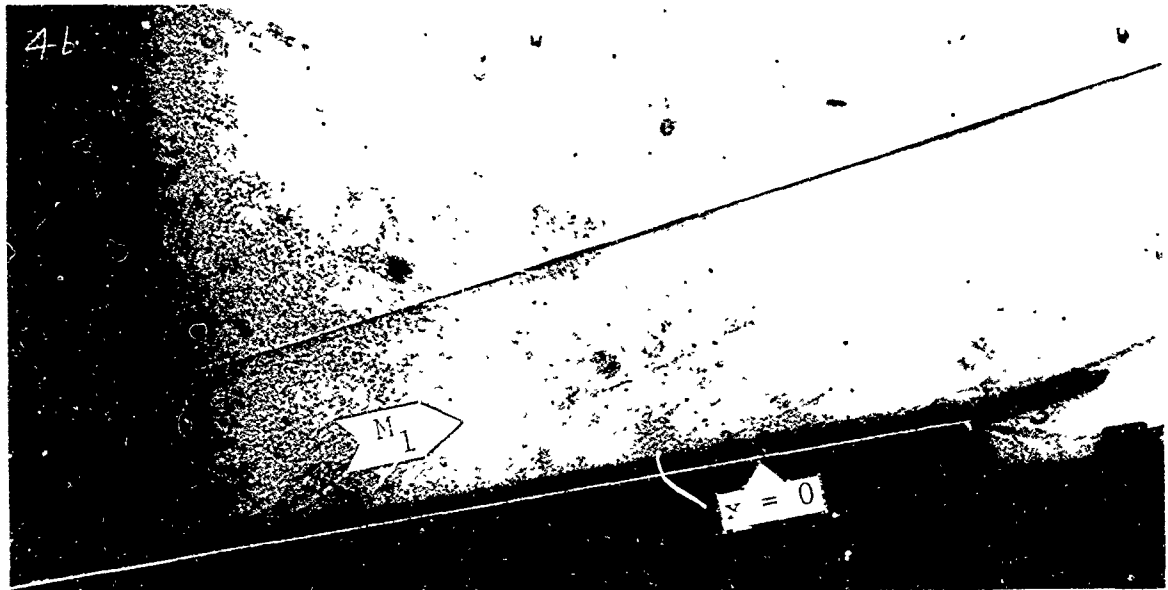
19

Figure 2   Coordinate System

20

Figure 3 Front View Photograph of Model Mounted on Injection System in Cabin Beneath Tunnel Test Section

21

a) M_1 5 04

b) M_1 - 4 75

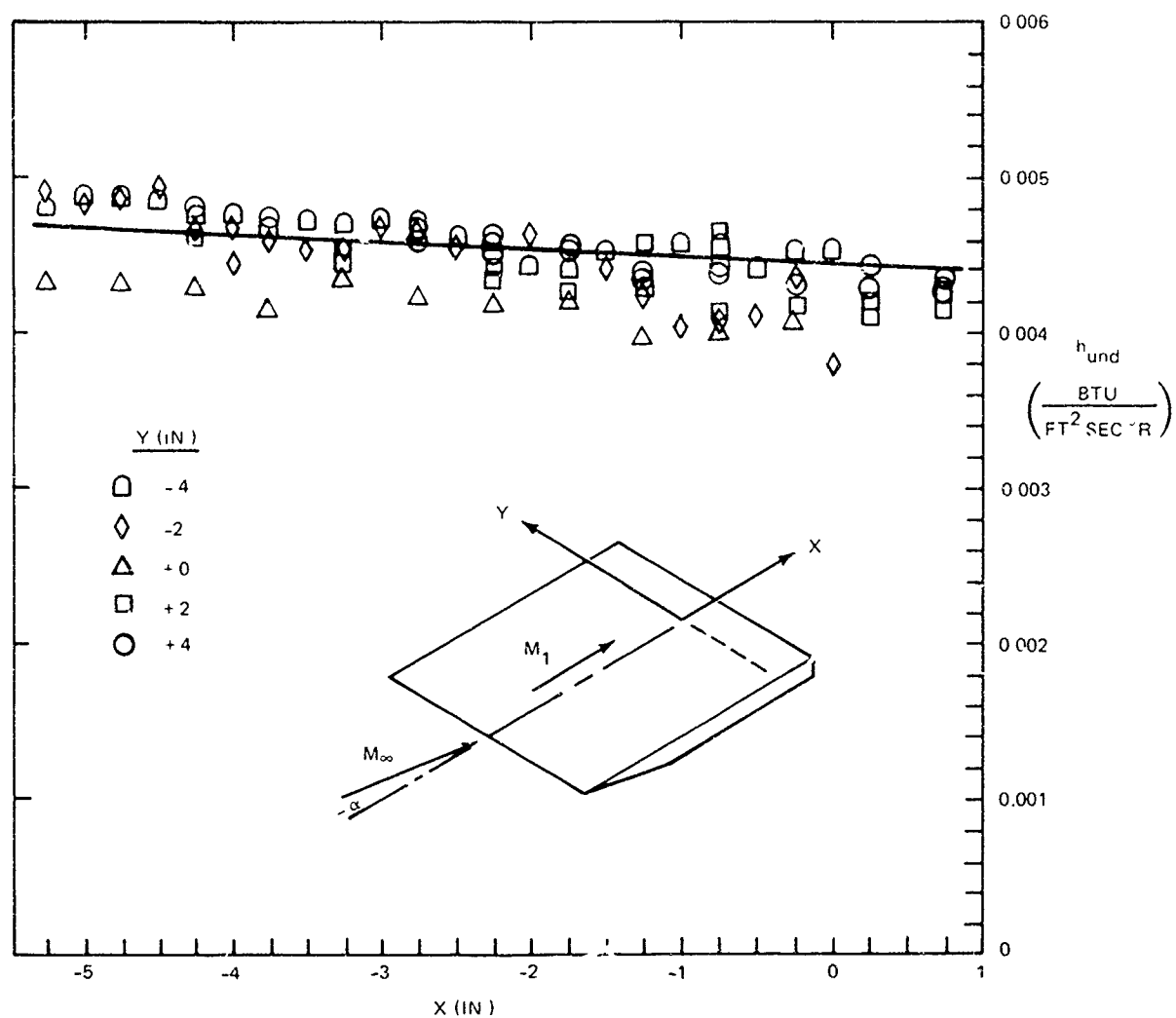Figure 4   Schlieren Photographs of Flows over Flat Plate Surface with no Step

Figure 5 Heat Transfer Coefficient Distributions on Flat Plate Surface with no Step for M_1 = 5.04 (α = -6.8°)

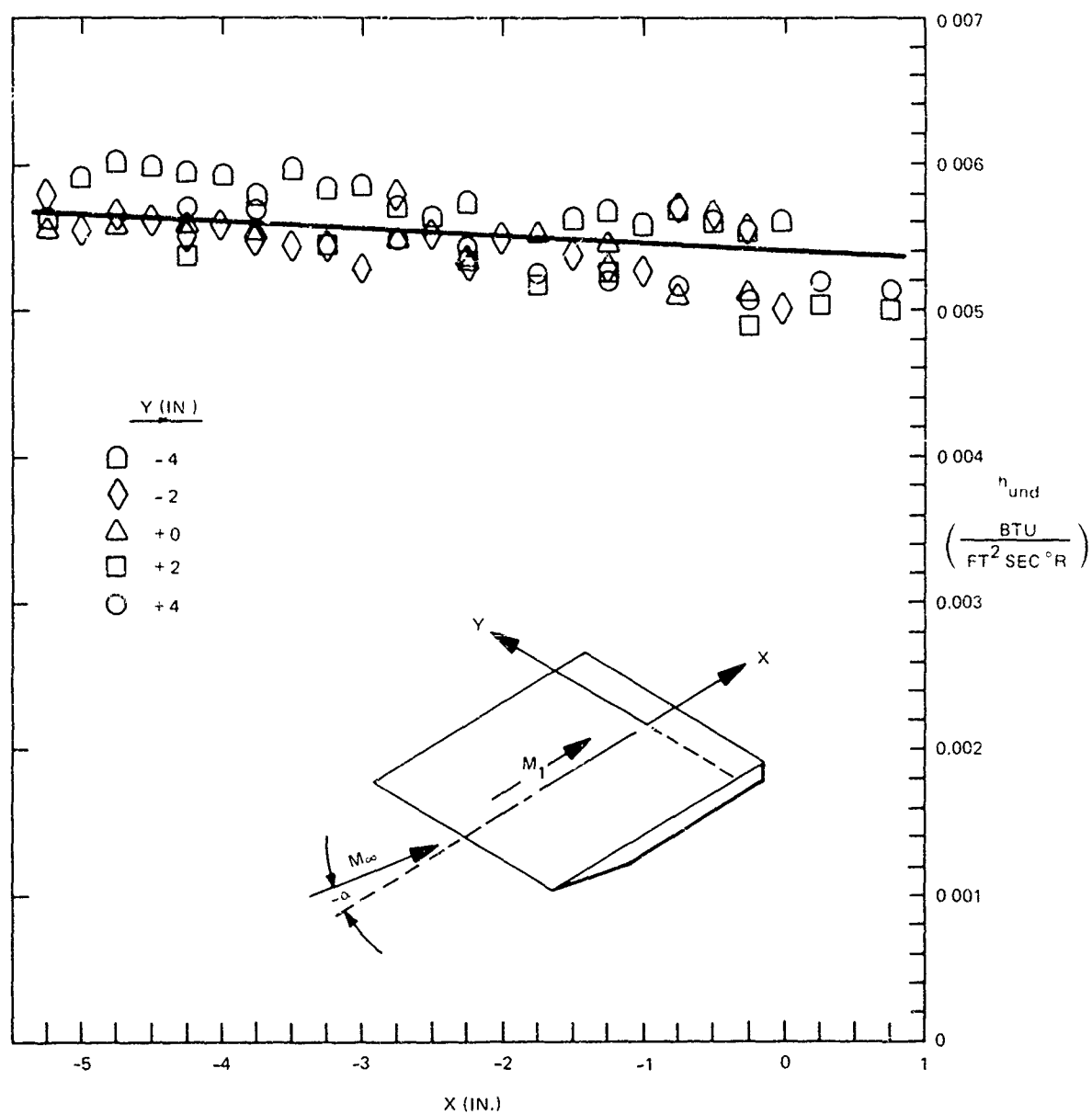Figure 6   Heat Transfer Coefficient Distributions on Flat Plate Surface with no Step for M_1 = 4.75 (α = -9.0°)

24

X	7.0	6.5	6.0	5.5	5.0	4.5	4.0	3.5	3.0	2.5	2.0	1.5	1.0	0.5	0.0	-0.5	-1.0	-1.5	-2.0	-2.5	-3.0	-3.5	-4.0	-4.5	-5.0	-5.5	r
0.75											0.92								0.92				0.95				0.75
0.50											0.92								0.92				0.96				0.50
0.25											0.90								0.90				0.93				0.25
0.00							1.04				0.94				0.94				0.86				0.95				0.00
-0.25							1.02				1.0				0.94				0.96				0.95				-0.25
-0.50							1.03				1.04				0.94				0.93				0.98				-0.50
-0.75							1.04				1.04				0.93				0.96				0.99				-0.75
-1.00							1.04				0.94				1.0												-1.00
-1.25							1.03				0.96				0.96				0.97								-1.25
-1.50							1.02				0.96				0.96								1.02				-1.50
-1.75							2.00								0.94								1.01				-1.75
-2.00							1.13				1.0				0.98												-2.00
-2.25							1.04				1.04				0.94												-2.25
-2.50							1.02				0.94				0.94												-2.50
-2.75							1.04																				-2.75
-3.00							1.05				0.94																-3.00
-3.25							1.06				0.94				0.98												-3.25
-3.50							1.07				0.97																-3.50
-3.75							1.04				0.97												1.02				-3.75
-4.00							1.05				0.94																-4.00
-4.25							1.66				0.94												1.01				-4.25
-4.50							1.07				1.0																-4.50
-4.75							1.07				0.96																-4.75
-5.00							1.05																				-5.00
-5.25							0.99				1.04				0.98												-5.25

M_1

Figure 7 Distribution of Heat Transfer Coefficient Ratios (h/h_{und}) on Flat Plate Surface for $M_1 = 5.04$, No Step Attached to Surface
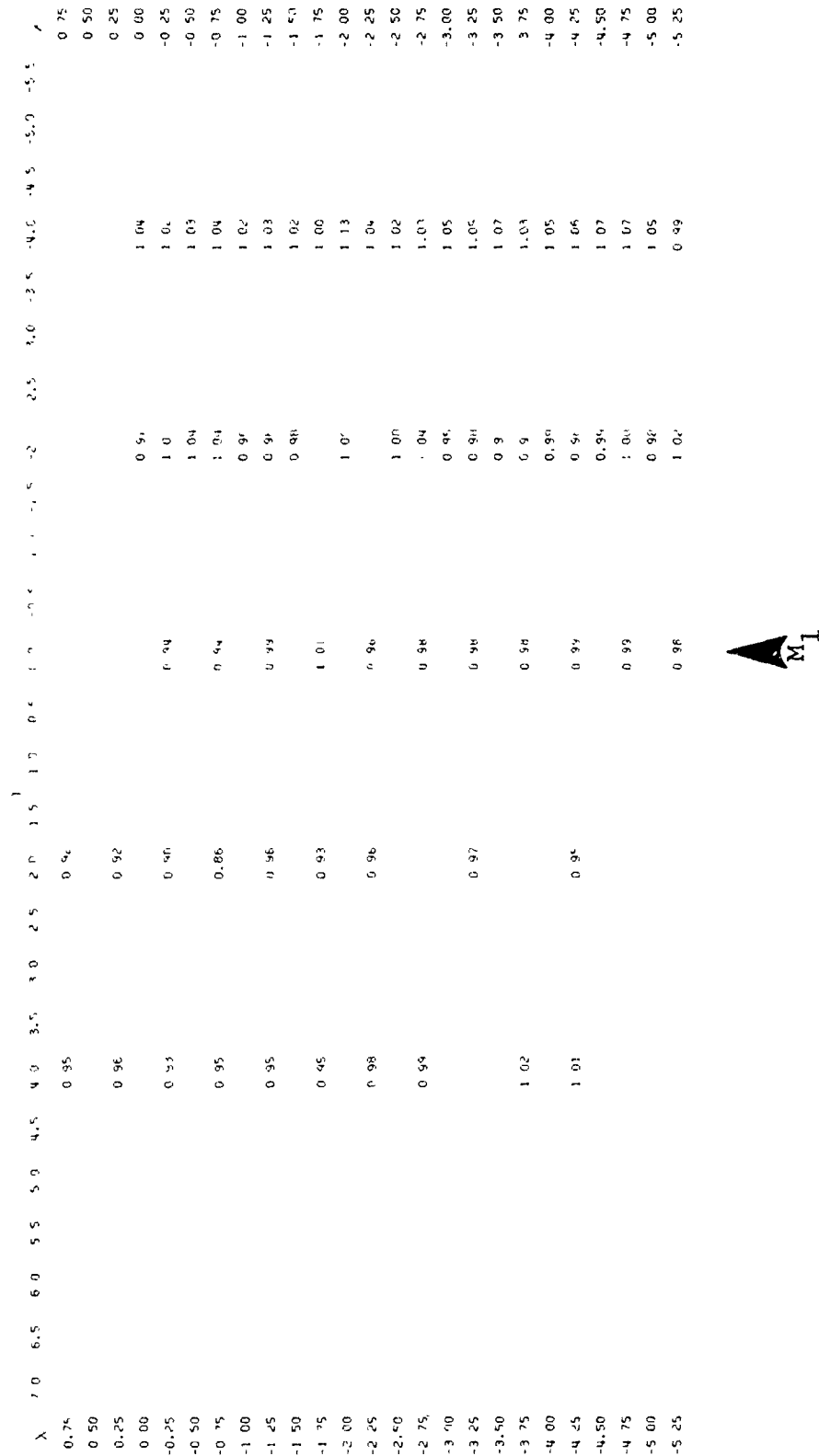
Figure 8   Distribution of Heat Transfer Coefficient Ratios (h/h_{und}) on Flat Plate Surface for M_1 = 4.75, No Step Attached to Surface

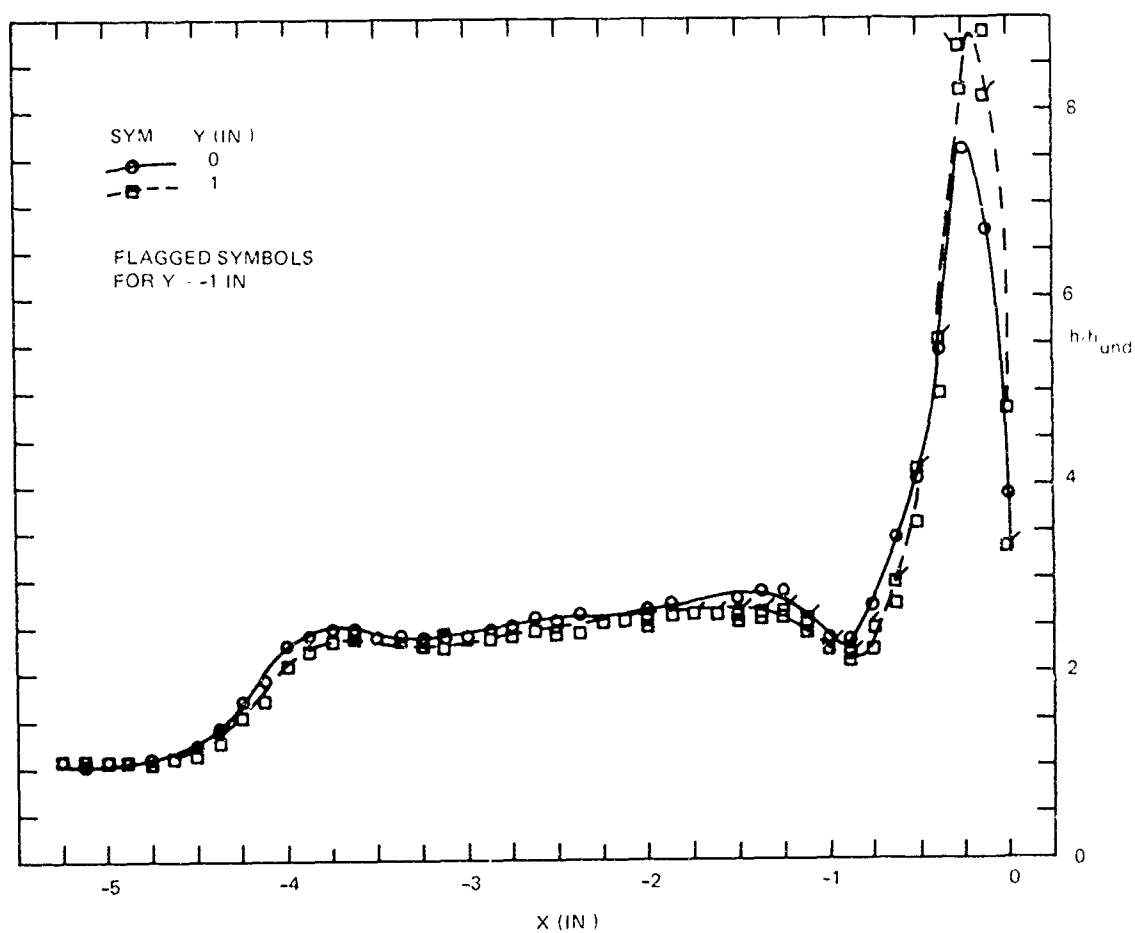Figure 9   Profile Schlieren Photograph of M_1 = 5.04 Flow Ahead of 3-inch Span Step

Figure 10   Streamwise Distributions of Heat Transfer Coefficient Ratios (h/h_{und}) on Plate Surface for M_1 = 5 04 Flow Ahead of 3-inch Span Step

27

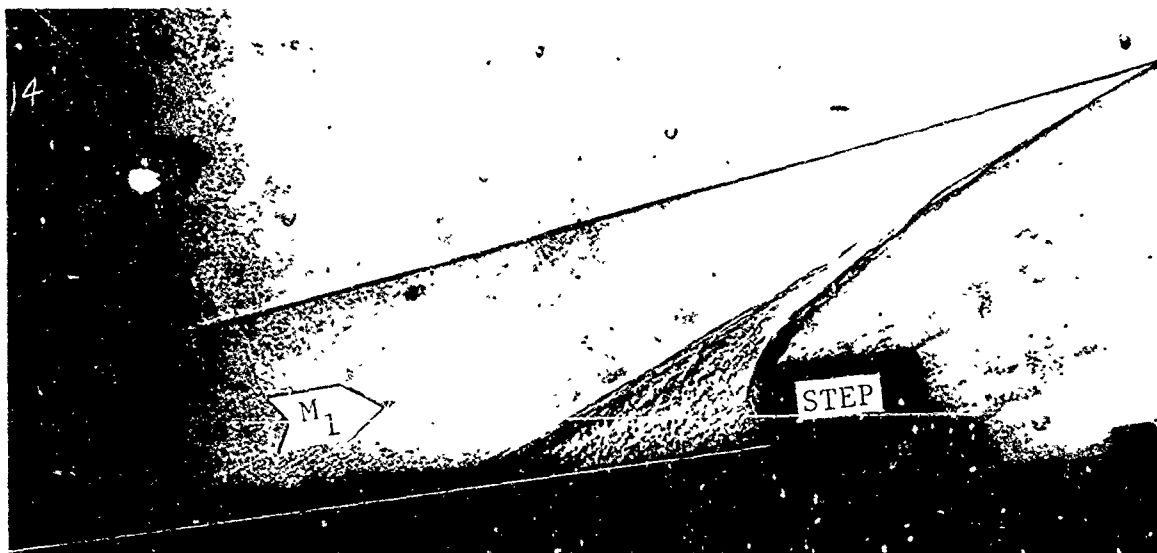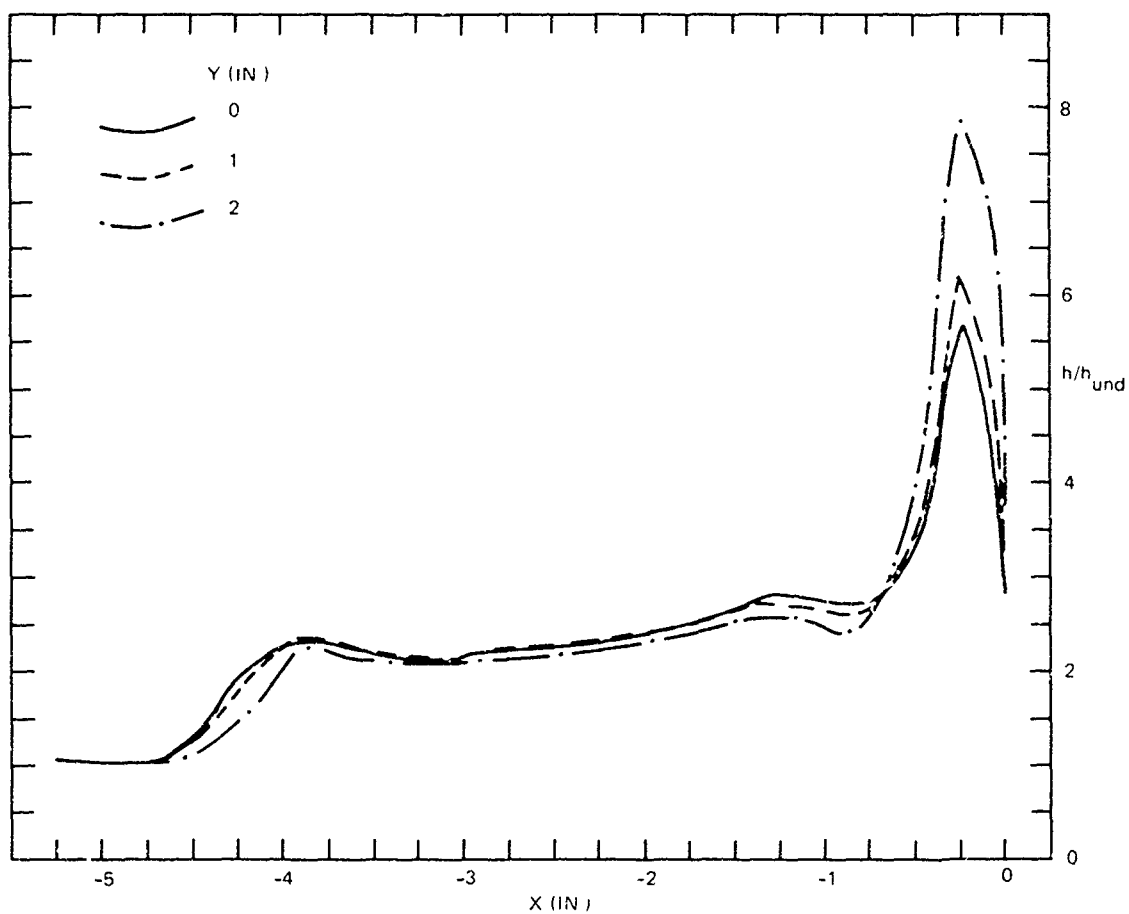Figure 11 — Frame from Motion Picture Showing Oil Film Flow on Surface Ahead of 3-inch Span Step for $M_1 = 5.04$
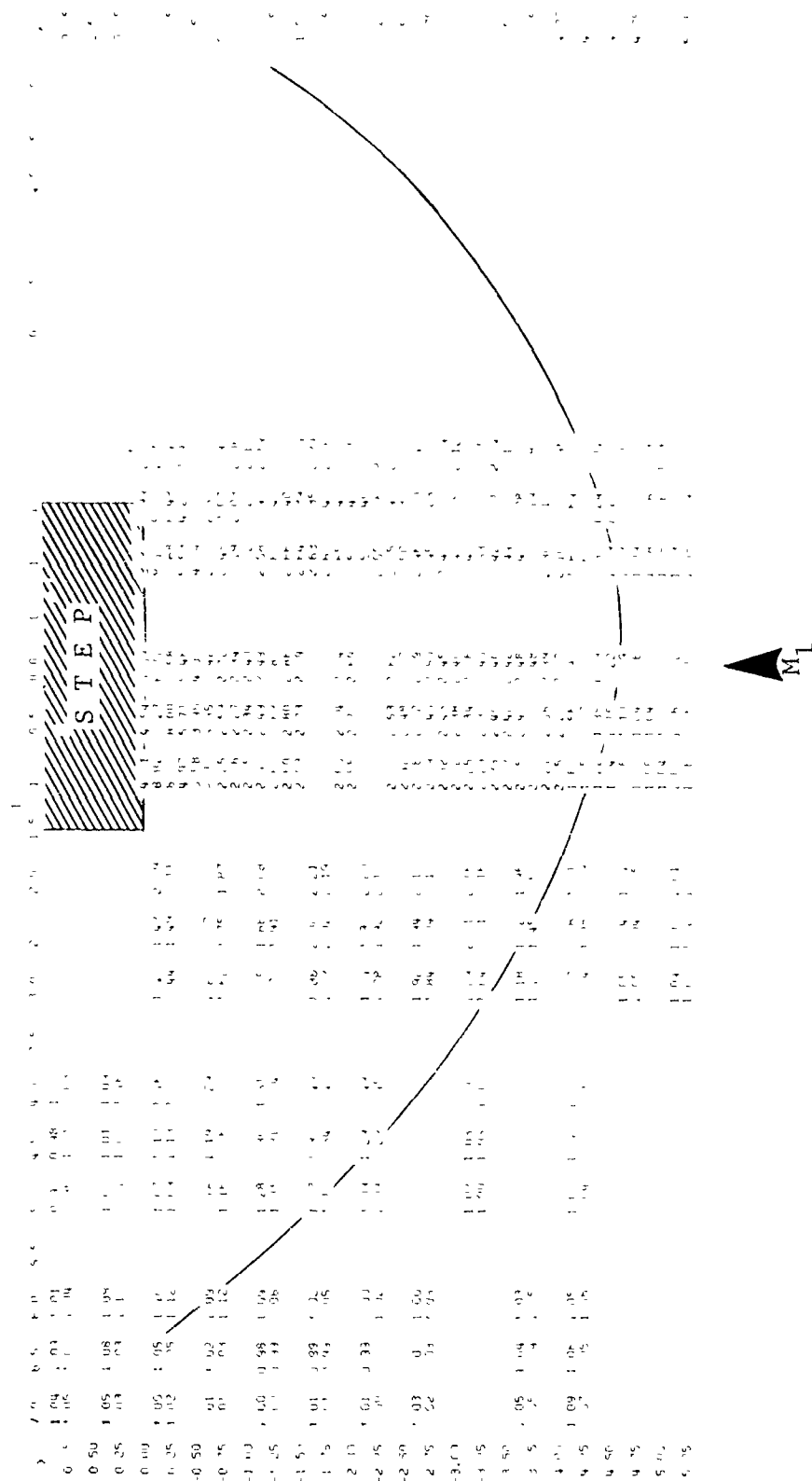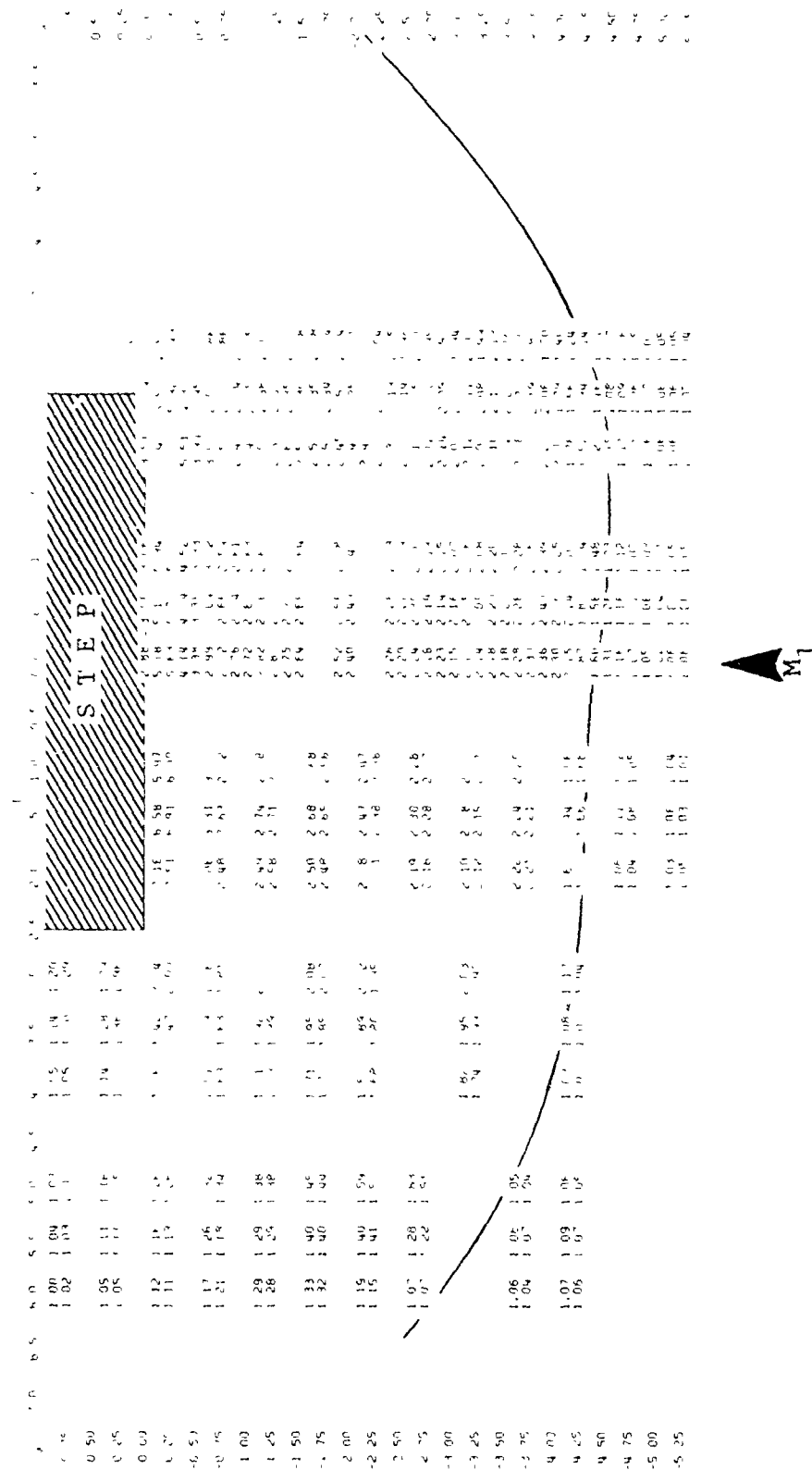
Figure 12 Distribution of Heat Transfer Coefficient Ratios (h/h_{und}) on Surface Ahead of 3-inch Span Step for $M_1 = 5.04$
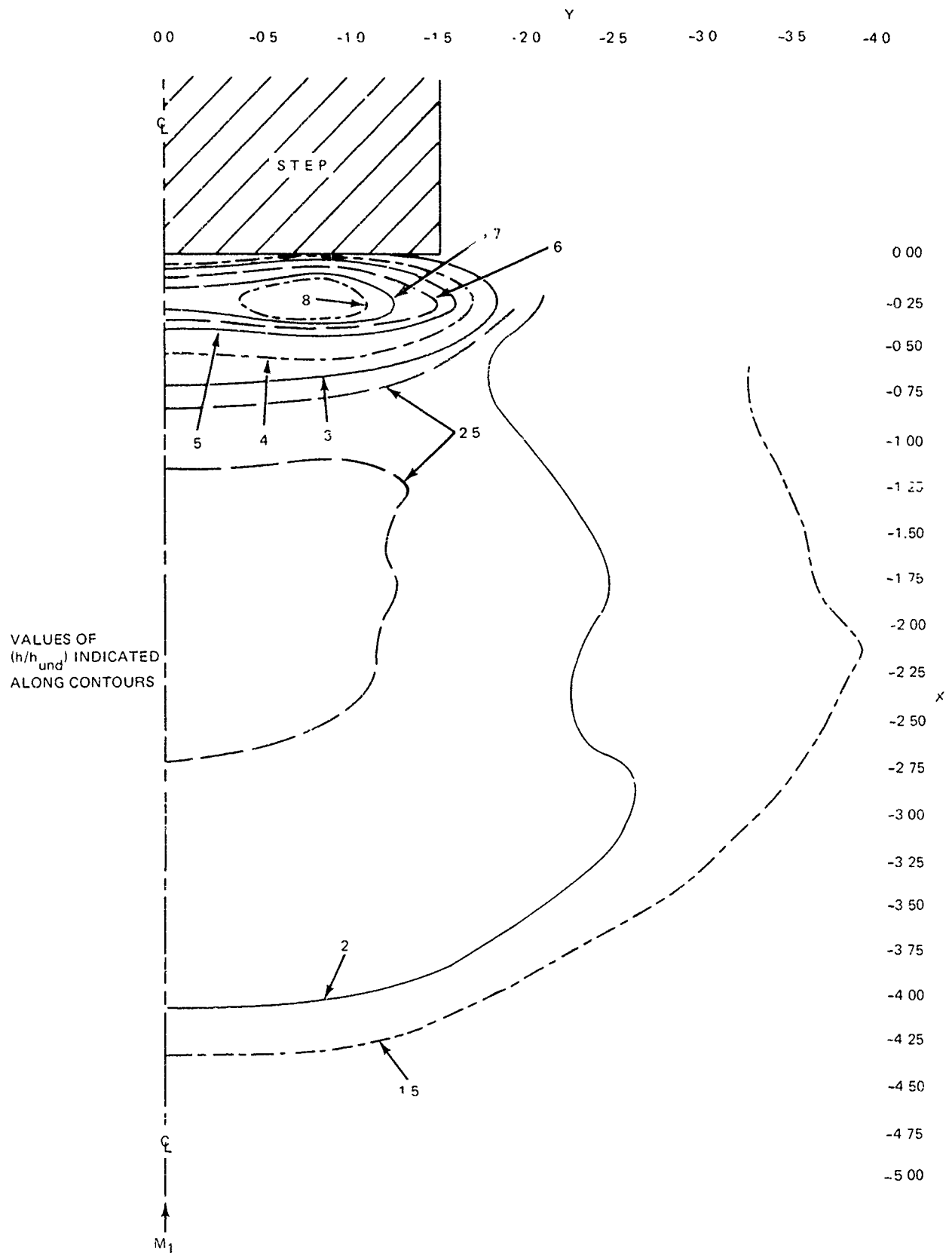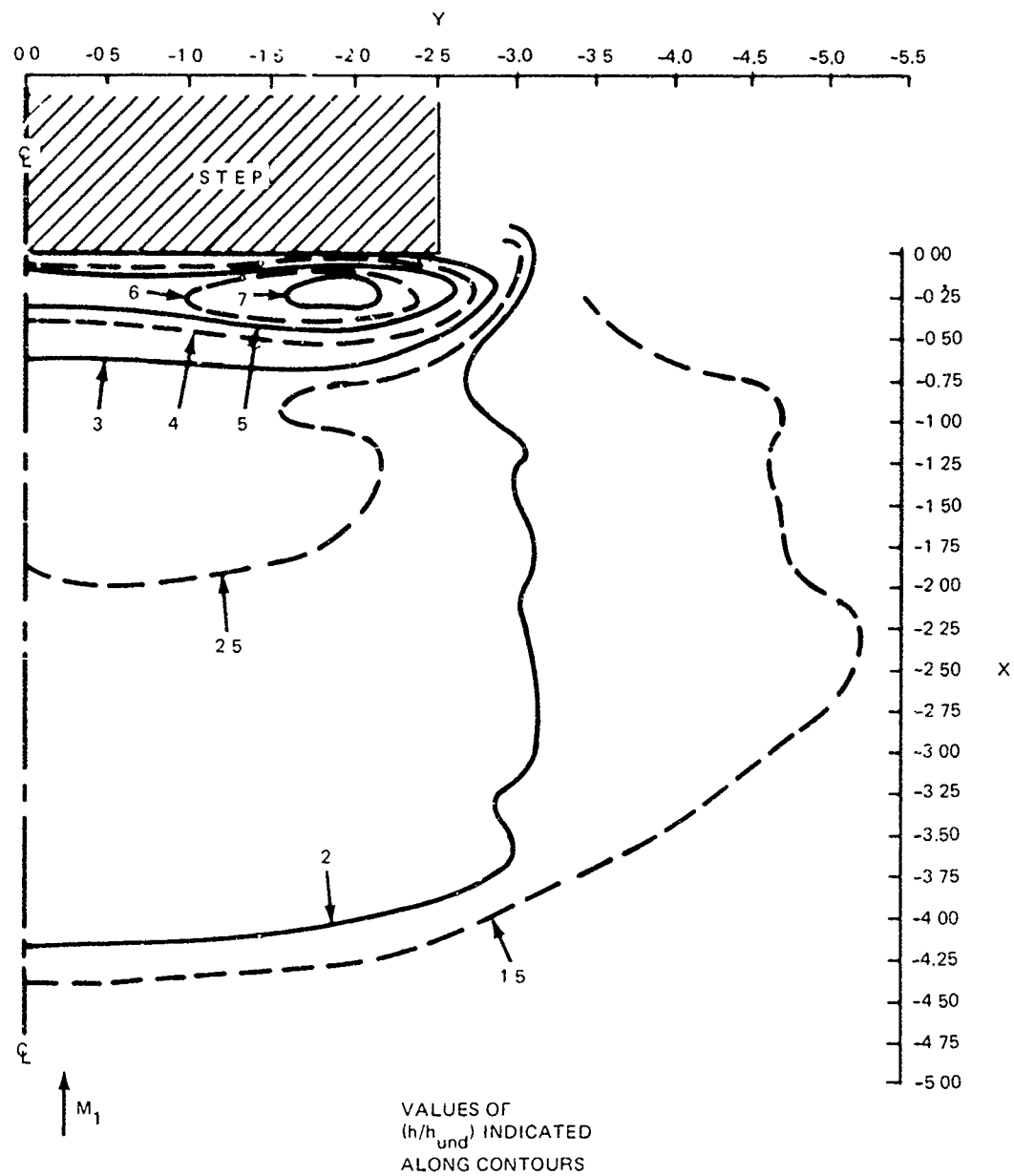
Figure 13   Lines of Constant (h/h_{und}) Contours on Surface Ahead of 3-inch Span Step for M_1 = 5.04
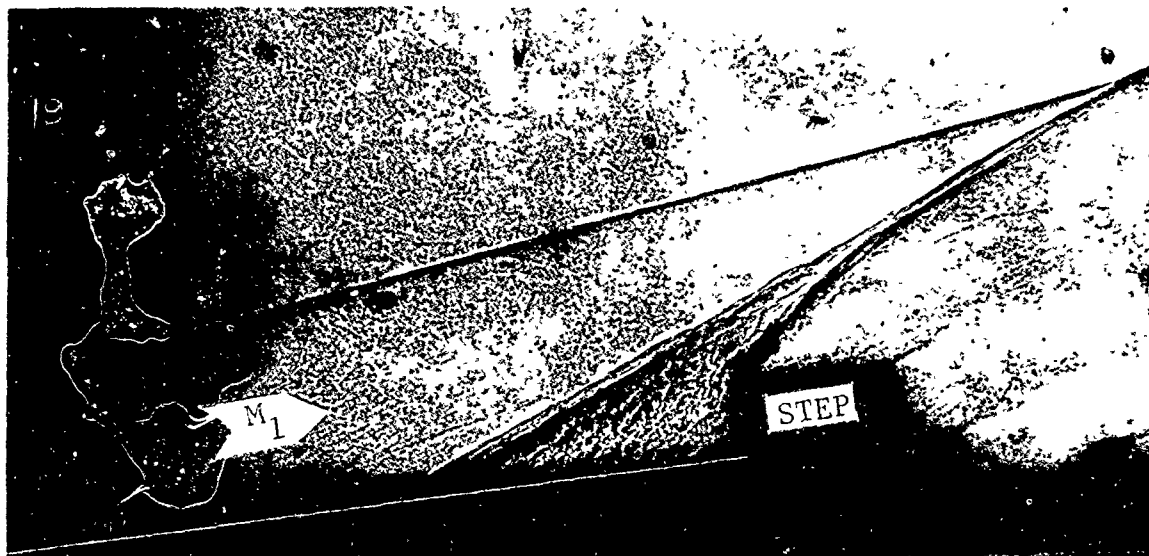
30

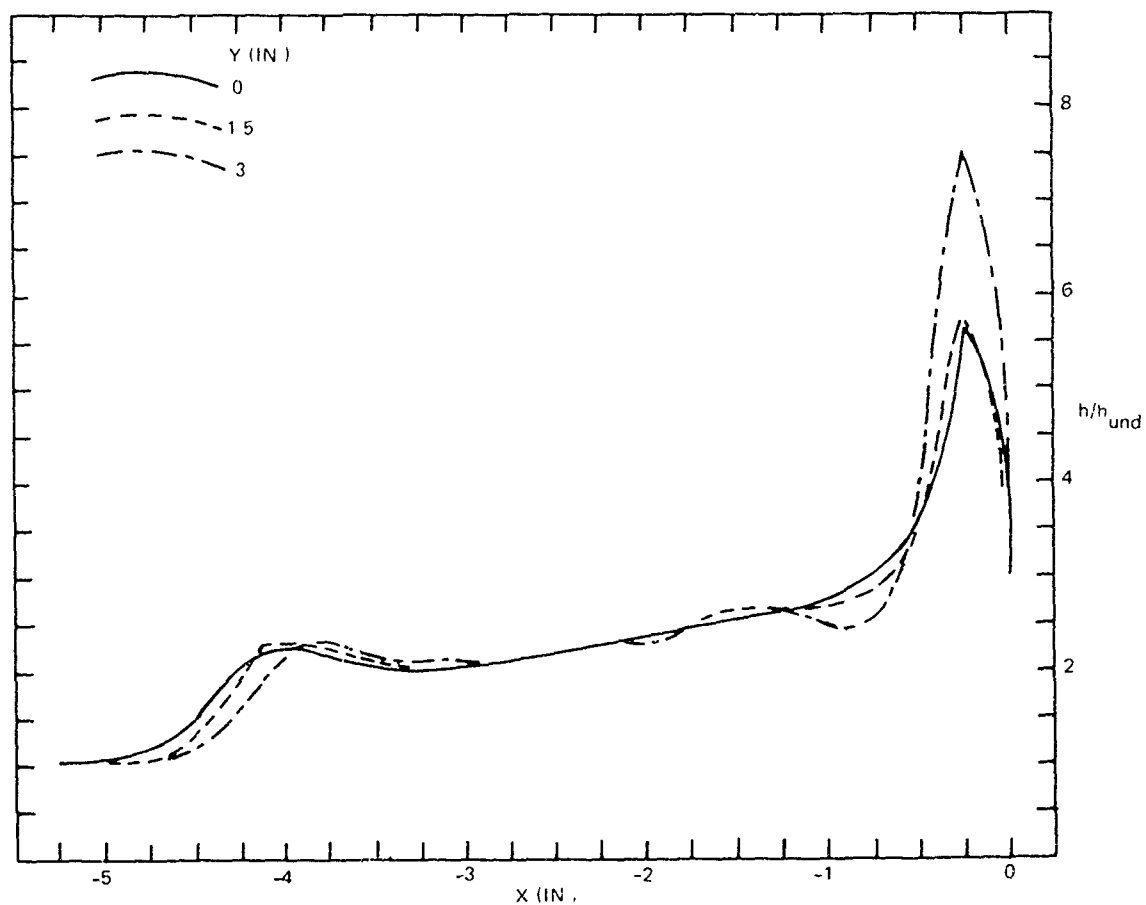Figure 14   Profile Schlieren Photograph of M_1 = 5.04 Flow Ahead of 5-inch Span Step

Figure 15 Streamwise Distributions of Heat Transfer Coefficient R   s (h/h_{und}) on Plate Surface for M_1 = 5.04 Flow Ahead of 5-inch Span Step

Figure 16   Frame from Motion Picture Showing Oil Film Flow on Surface Ahead of 5-inch Span Step for $M_1 = 5.04$
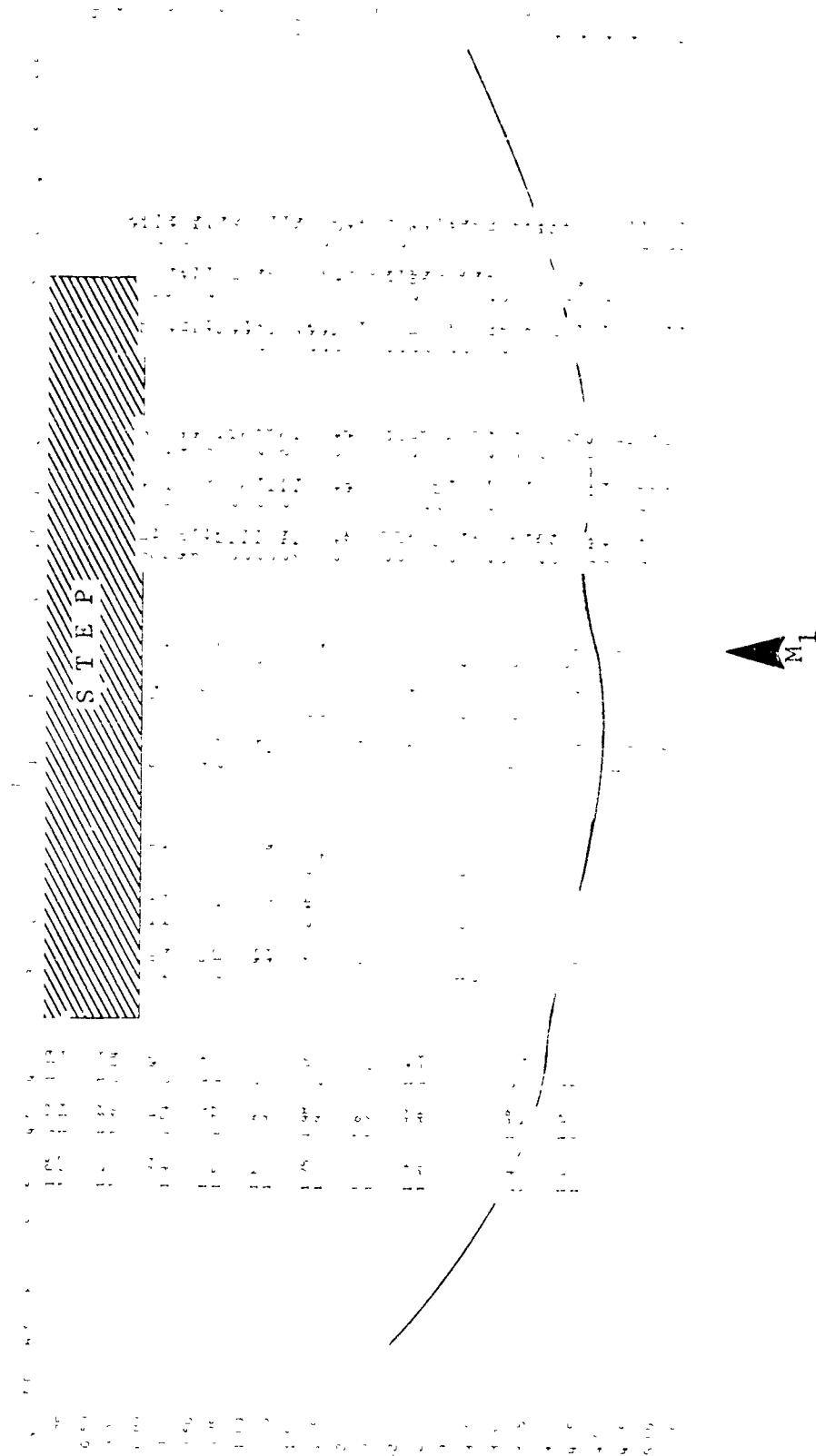
Figure 17   Distribution of Heat Transfer Coefficient Ratios on Surface Ahead of 5-inch Span Step for M_1 = 5.04
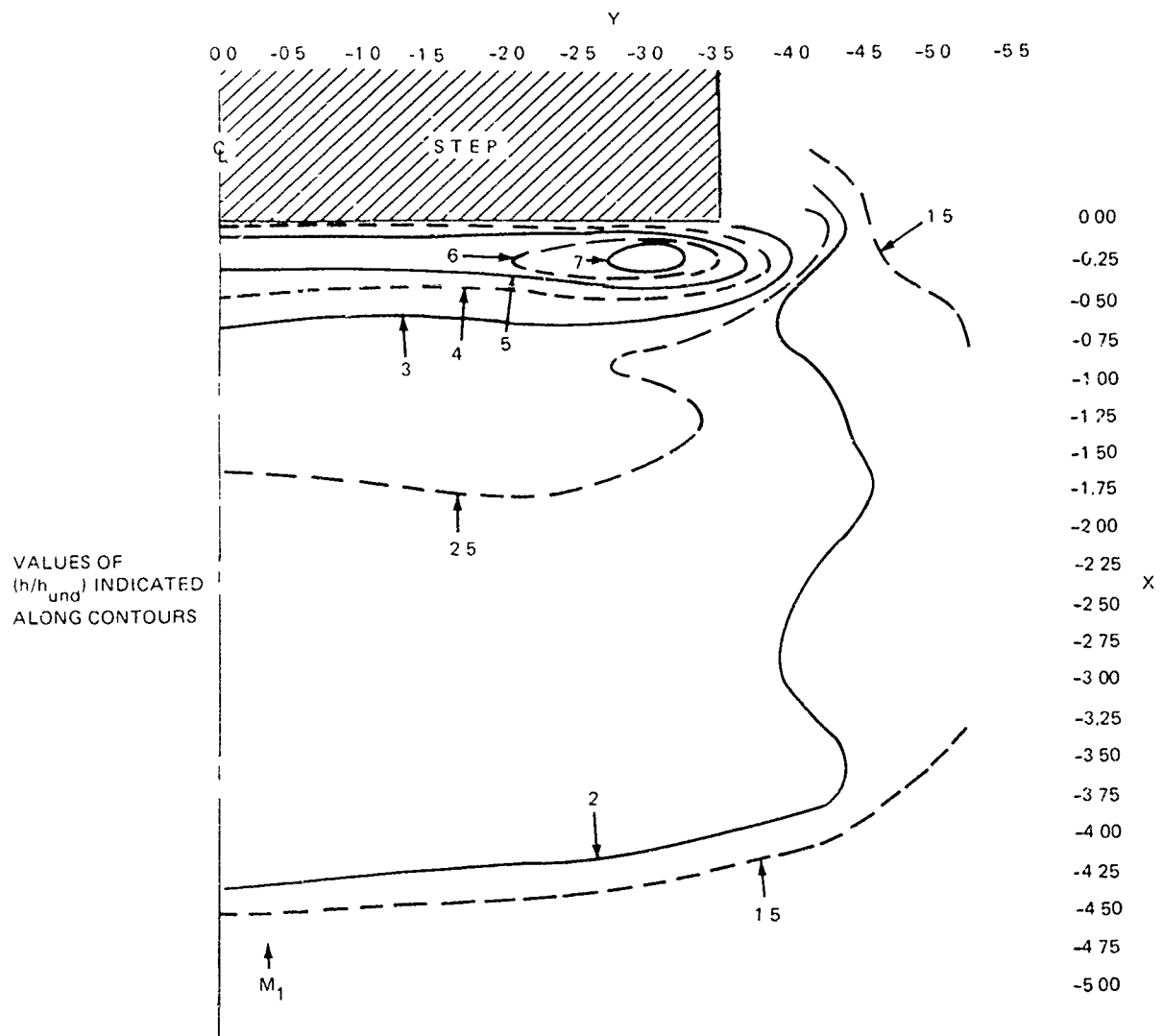
Figure 18   Lines of Constant (h/h_{und}) Contours on Surface Ahead of 5-inch Span Step for $M_1 = 5.04$

Figure 19   Profile Schlieren Photograph of M_1 = 5 04 Flow Ahead of 7-inch Span Step

Figure 20   Streamwise Distributions of Heat Transfer Coefficient Ratios on Plate Surface for M_1 = 5.04 Flow
Ahead of 7-inch Span Step

35

Figure 21 Frame from Motion Picture Showing Oil Film Flow on Surface Ahead of 7-inch Span Step for $M_1 = 5\,04$

Figure 22   Distribution of Heat Transfer Coefficient Ratios on Surface Ahead of 7-inch Span Step for $M_1 = 5.04$

Figure 23   Lines of Constant (h/h_{und}) Contours on Surface Ahead of 7-inch Span Step for $M_1 = 5.04$
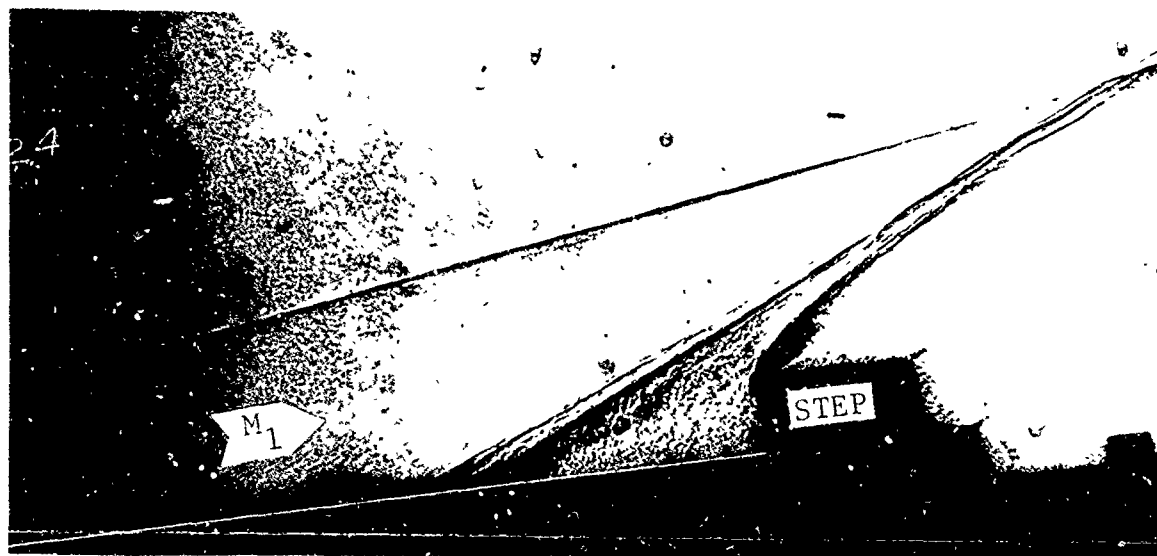
38

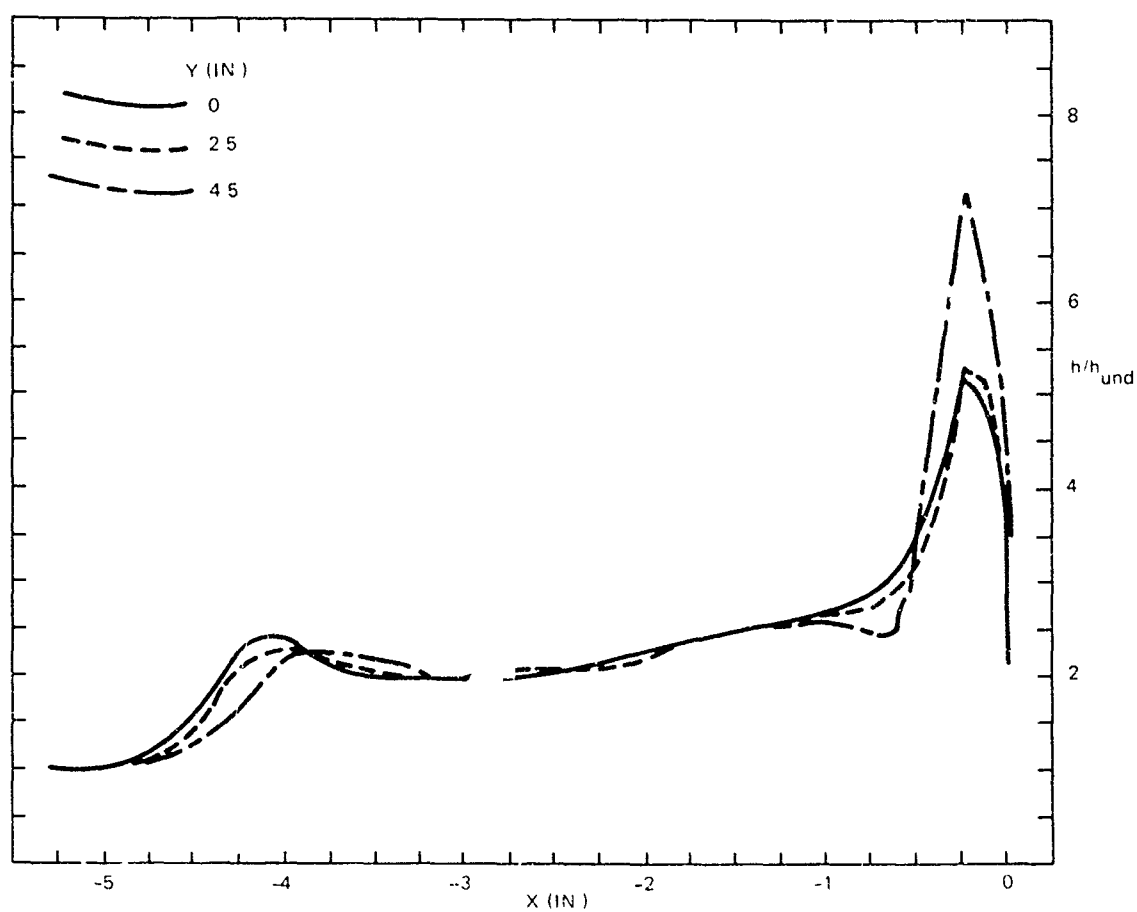Figure 24 Profile Schlieren Photograph of M_1 = 5.04 Flow Ahead of 10-inch Span Step

Figure 25   Streamwise Distributions of Heat Transfer Coefficient Ratios on Plate Surface for M_1 = 5.04
Flow Ahead of 10-inch Span Step

39

Figure 26 Frame from Motion Picture Showing Oil Film Flow on Surface Ahead of 10 inch Span Step for $M_1 = 5.04$
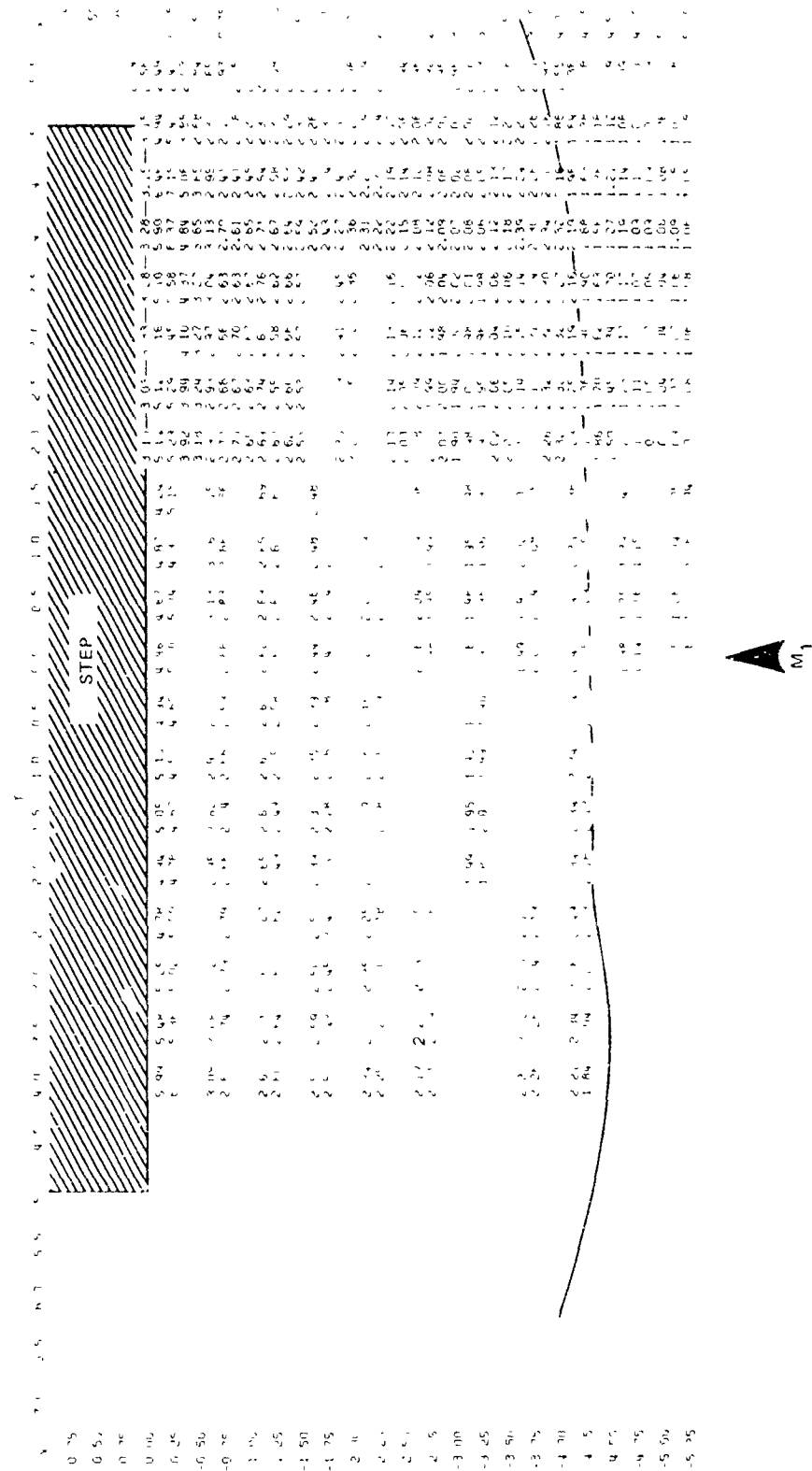
Figure 27 Distribution of Heat Transfer Coefficient Ratios on Surface Ahead of 10-inch Span Step for $M_1 = 5.04$
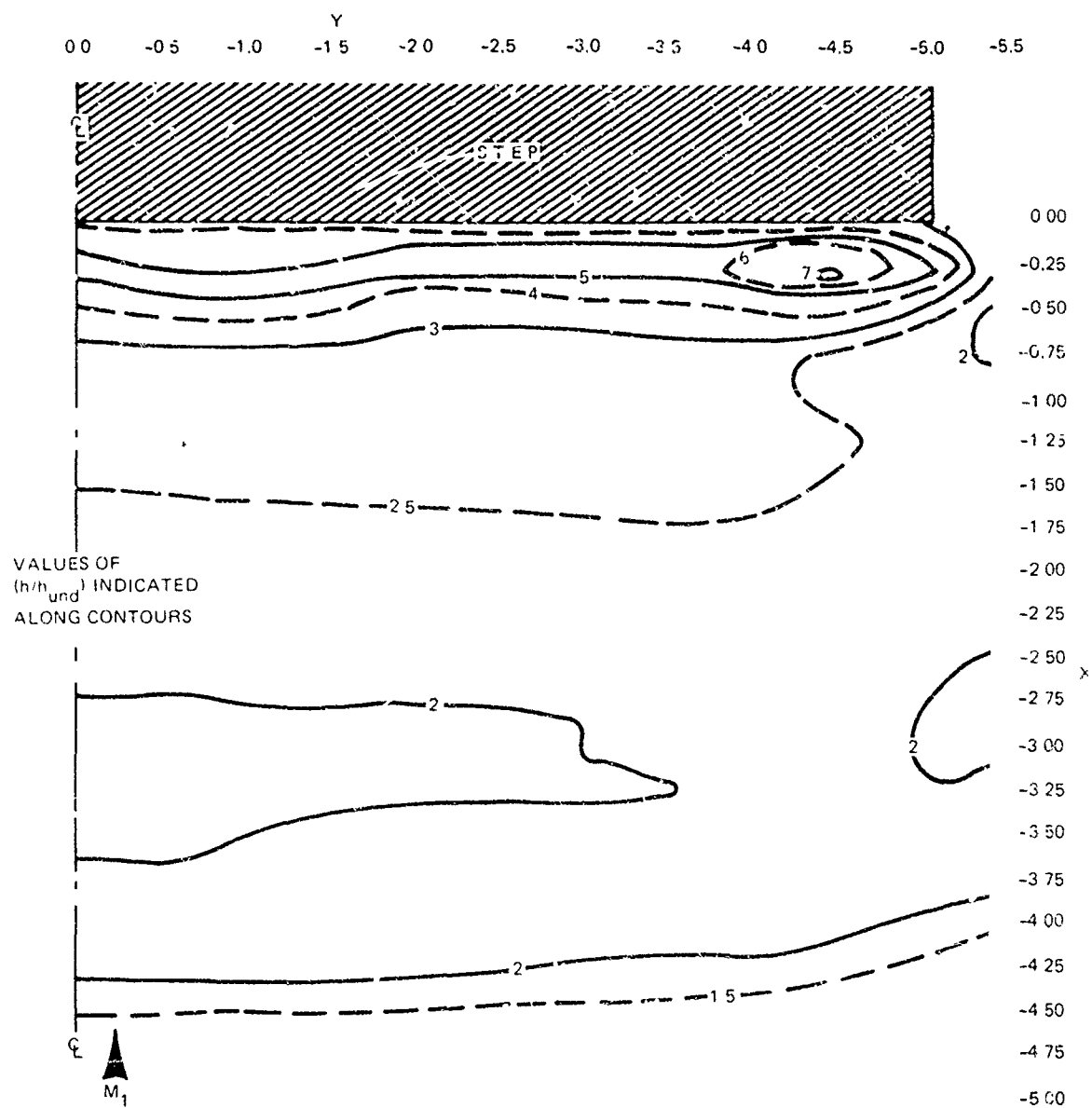
41

Figure 28   Lines of Constant (h/h_{und}) Contours on Surface Ahead of 10-inch Span Step for $M_1 = 5.04$

42

Figure 29   Profile Schlieren Photograph of M_1 = 4.75 Flow Ahead of 3-inch Span Step
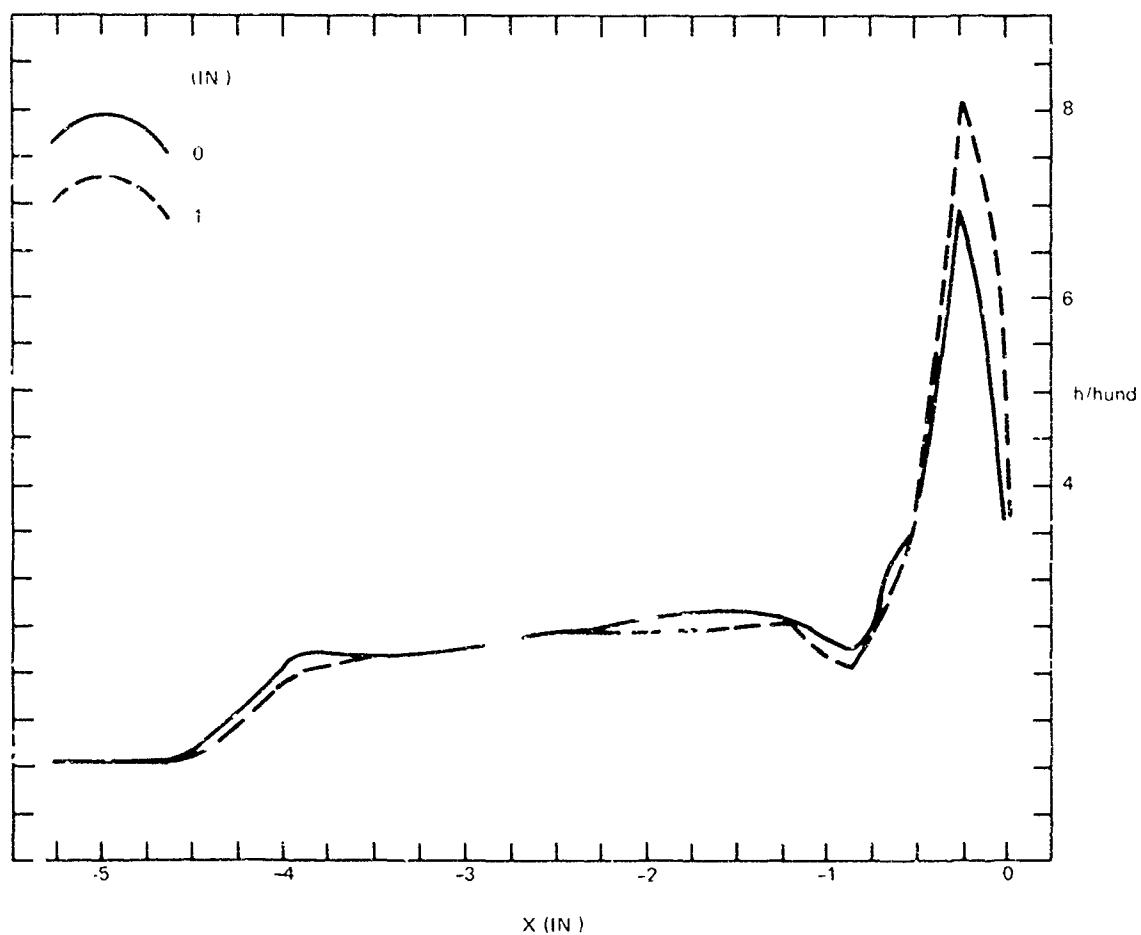

Figure 30   Streamwise Distributions of Heat Transfer Coefficient Ratios (h/h_{und}) on Plate Surface for M_1 = 4.75 Flow Ahead of 3-inch Span Step
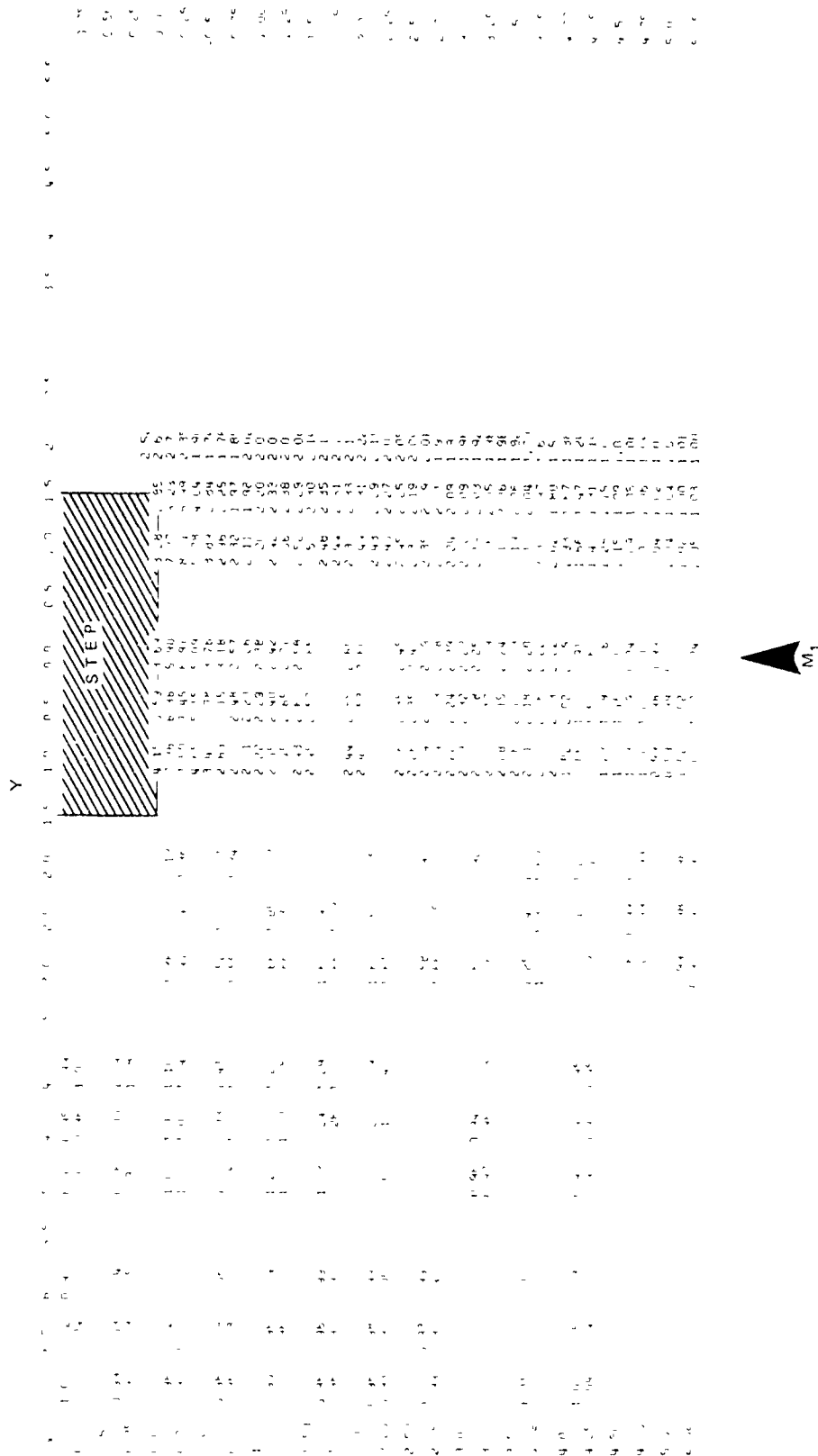
43

Figure 31   Distribution of Heat Transfer Coefficient Ratios (h/h_und) on Surface Ahead of 3-inch Span Step for $M_1 = 4.75$
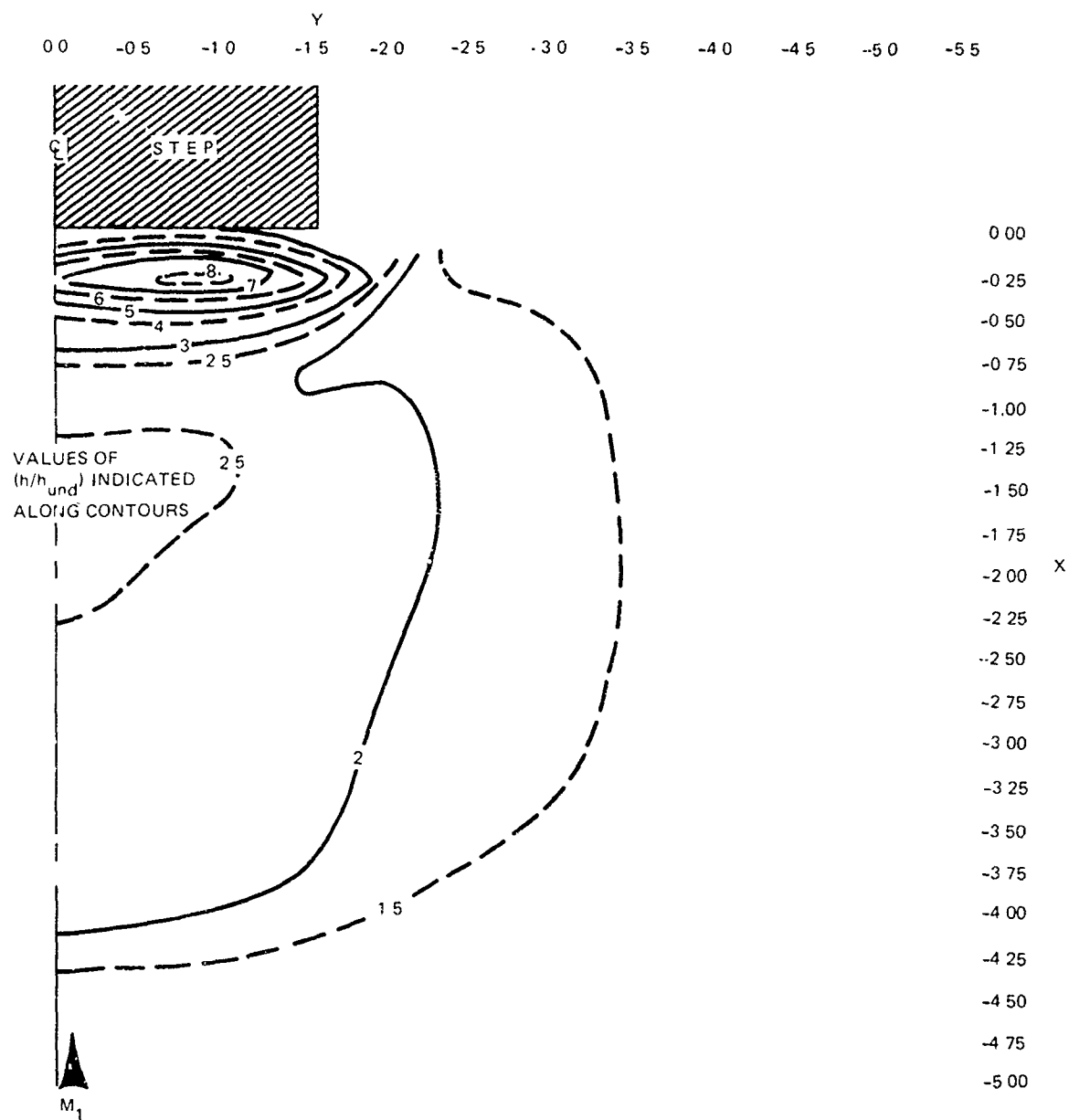
Figure 32   Lines of Constant (h/h_{und}) Contours on Surface Ahead of 3-inch Span Step for M_1 = 4.75

45

Figure 33   Profile Schlieren Photograph of $M_1 = 4.75$ Flow Ahead of 5-inch Span Step

Figure 34   Streamwise Distributions of Heat Transfer Coefficient Ratios on Plate Surface for $M_1 = 4.75$ Flow Ahead of 5-inch Span Step

46

Figure 35   Distribution of Heat Transfer Coefficient Ratios on Surface Ahead of 5-inch Span Step for $M_1 = 4.75$

47

Figure 36 Lines of Constant (h/h_{und}) Contours on Surface Ahead of 5-inch Span Step for $M_1 = 4.75$

48

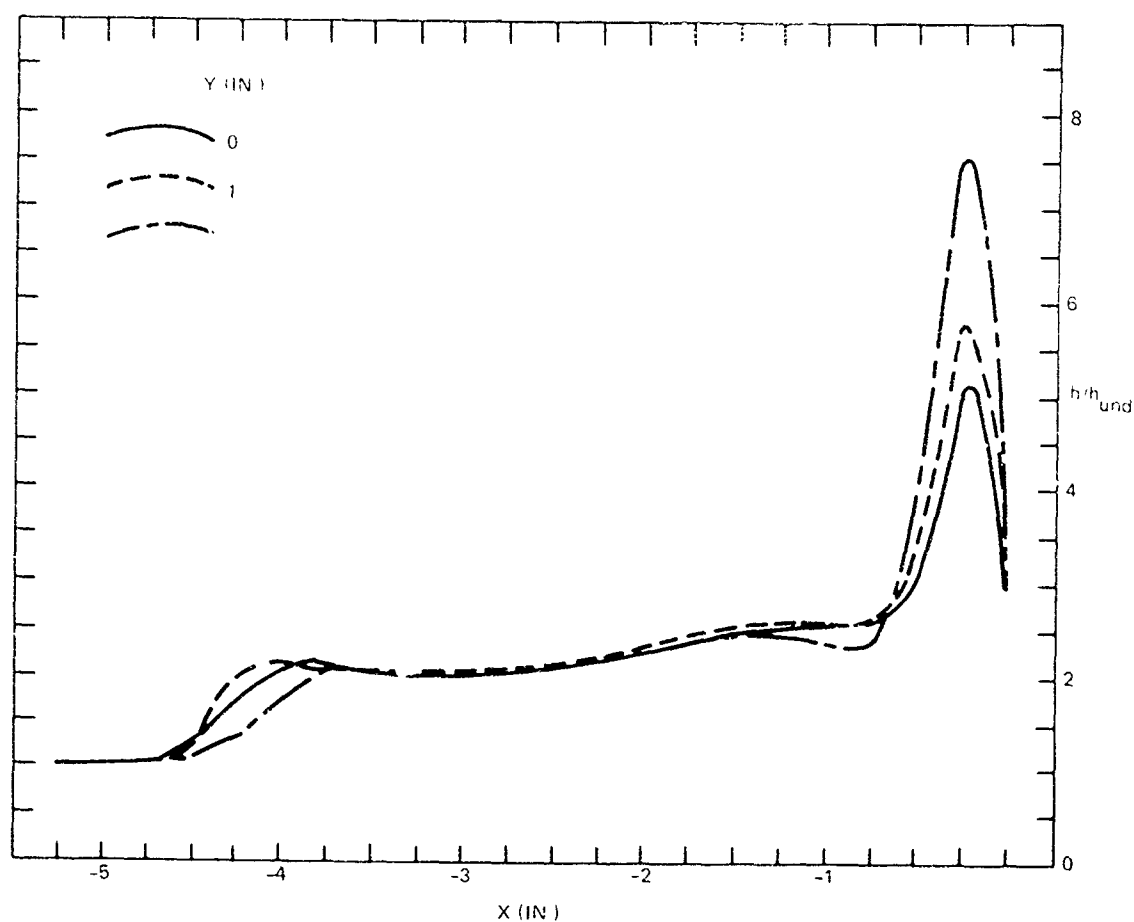Figure 37   Profile Schlieren Photograph of M_1 = 4.75 Flow Ahead of 7-inch Span Step

Figure 38   Streamwise Distributions of Heat Transfer Coefficient Ratios on Plate Surface for M_1 = 4.75 Flow Ahead of 7-inch Span Step.
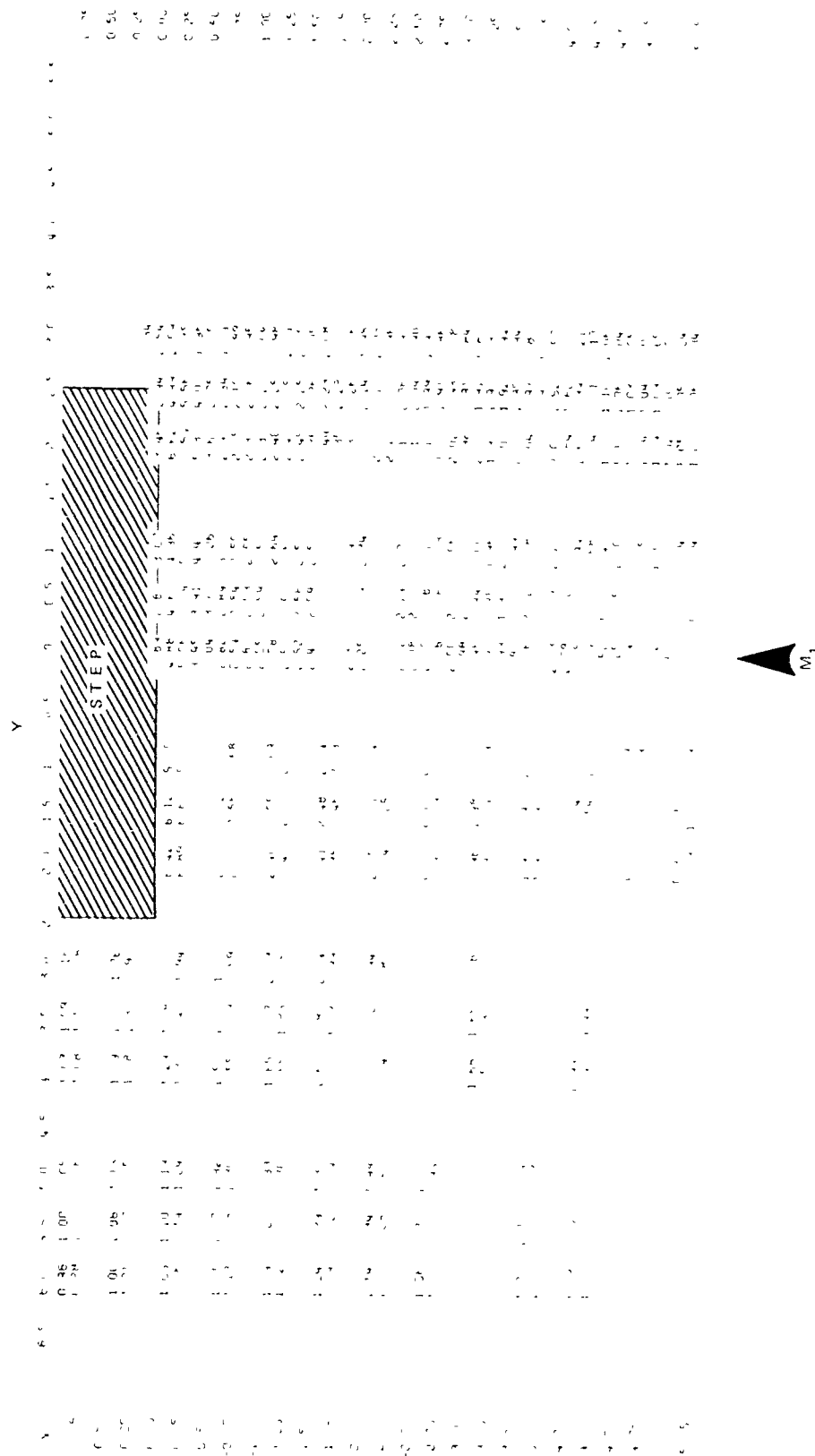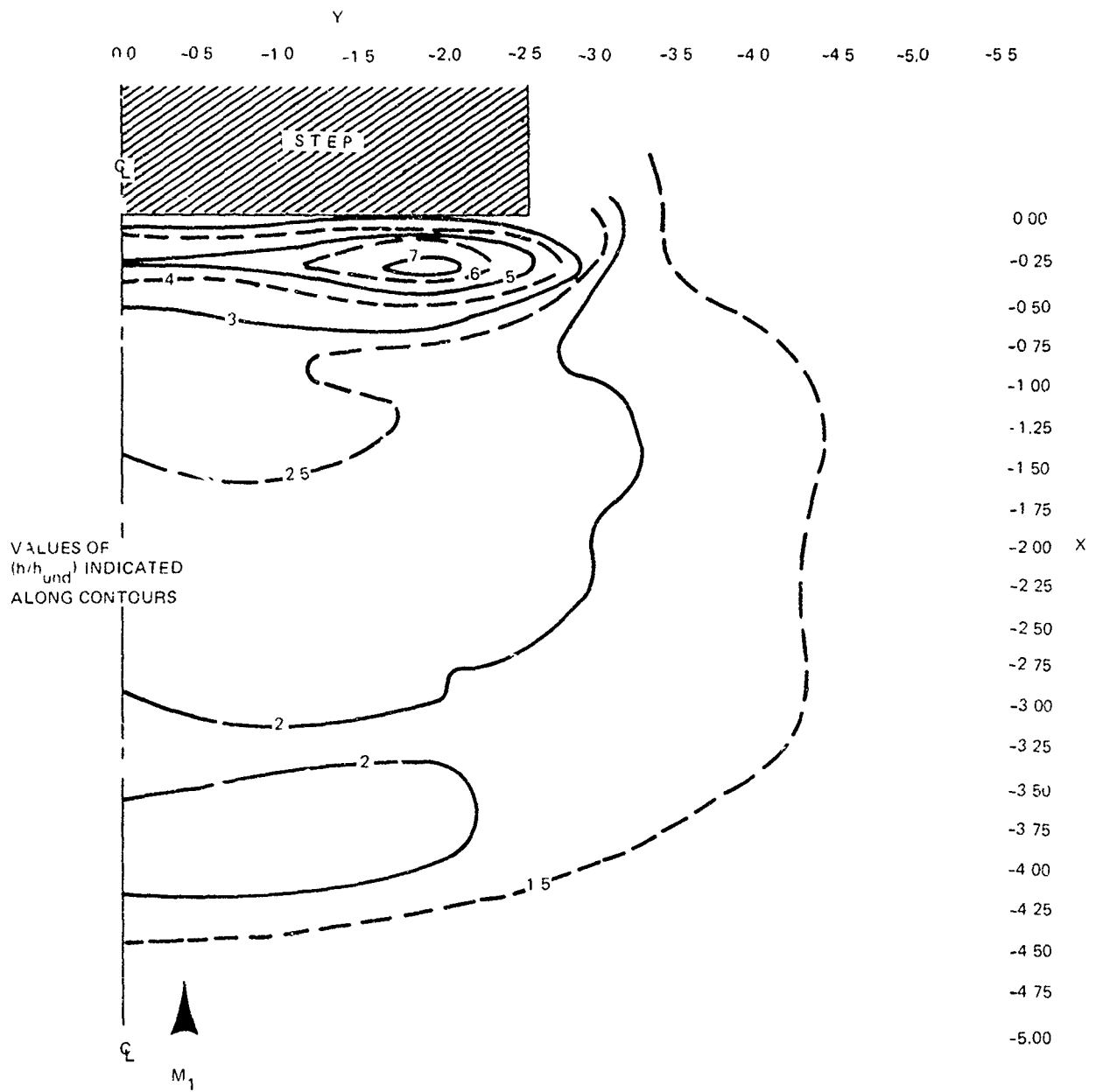
49

Figure 39   Distribution of Heat Transfer Coefficient Ratios on Surface Ahead of 7-inch Span Step for M_1 = 4.75
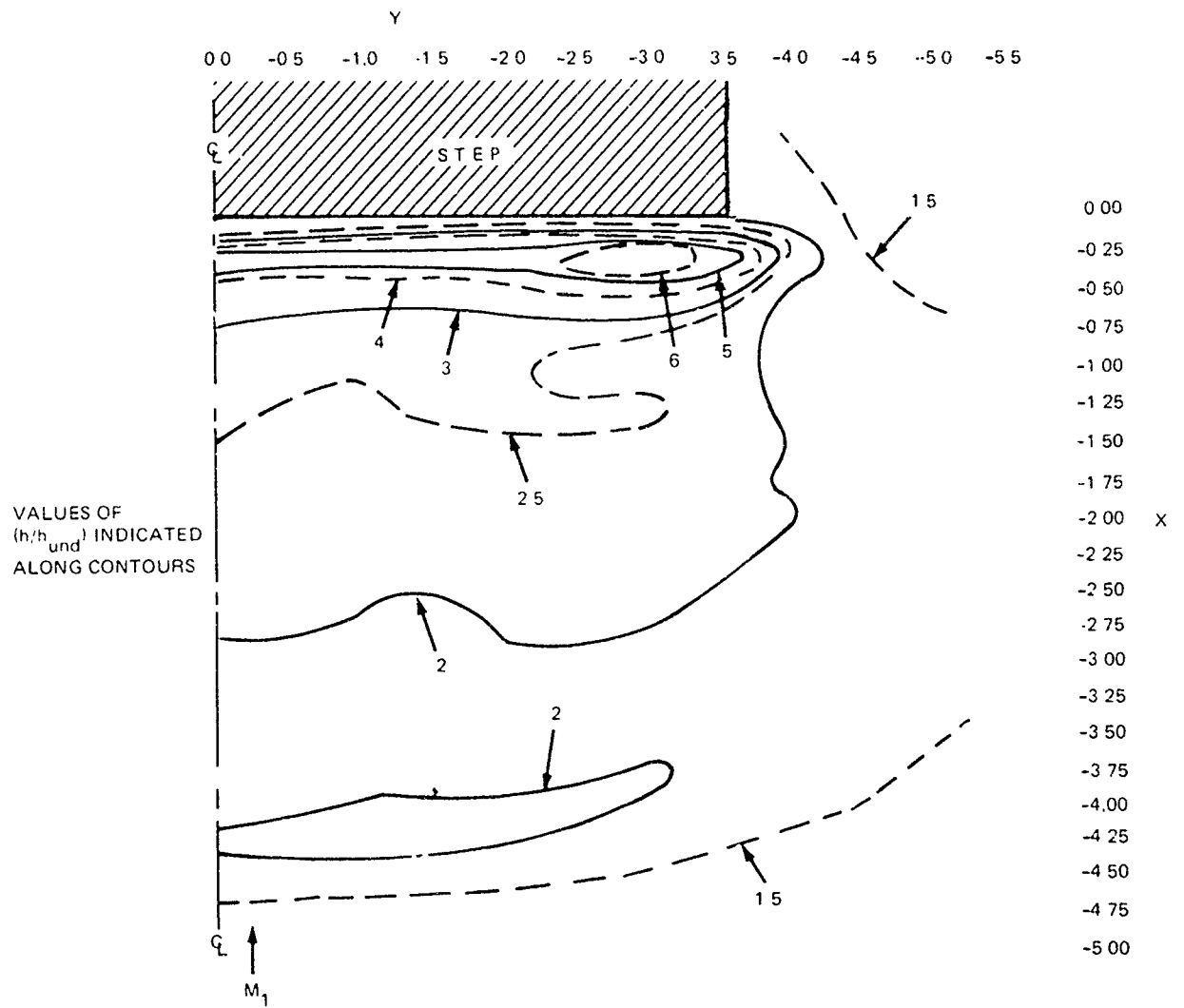
Figure 40   Lines of Constant (h/h$_{und}$) Contours on Surface Ahead of 7-inch Span Step for M$_1$ = 4 75

51

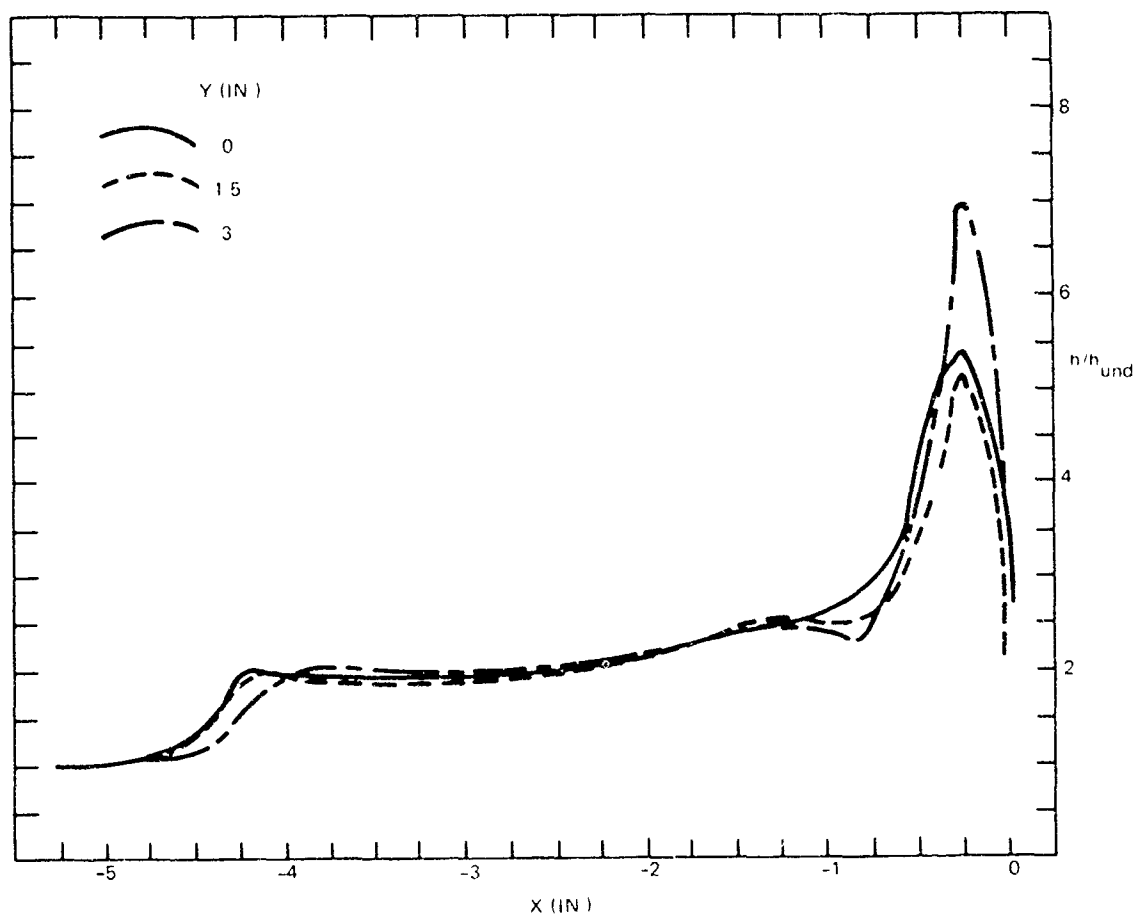Figure 41   Profile Schlieren Photograph of M_1 = 4.75 Flow Ahead of 10-inch Span Step
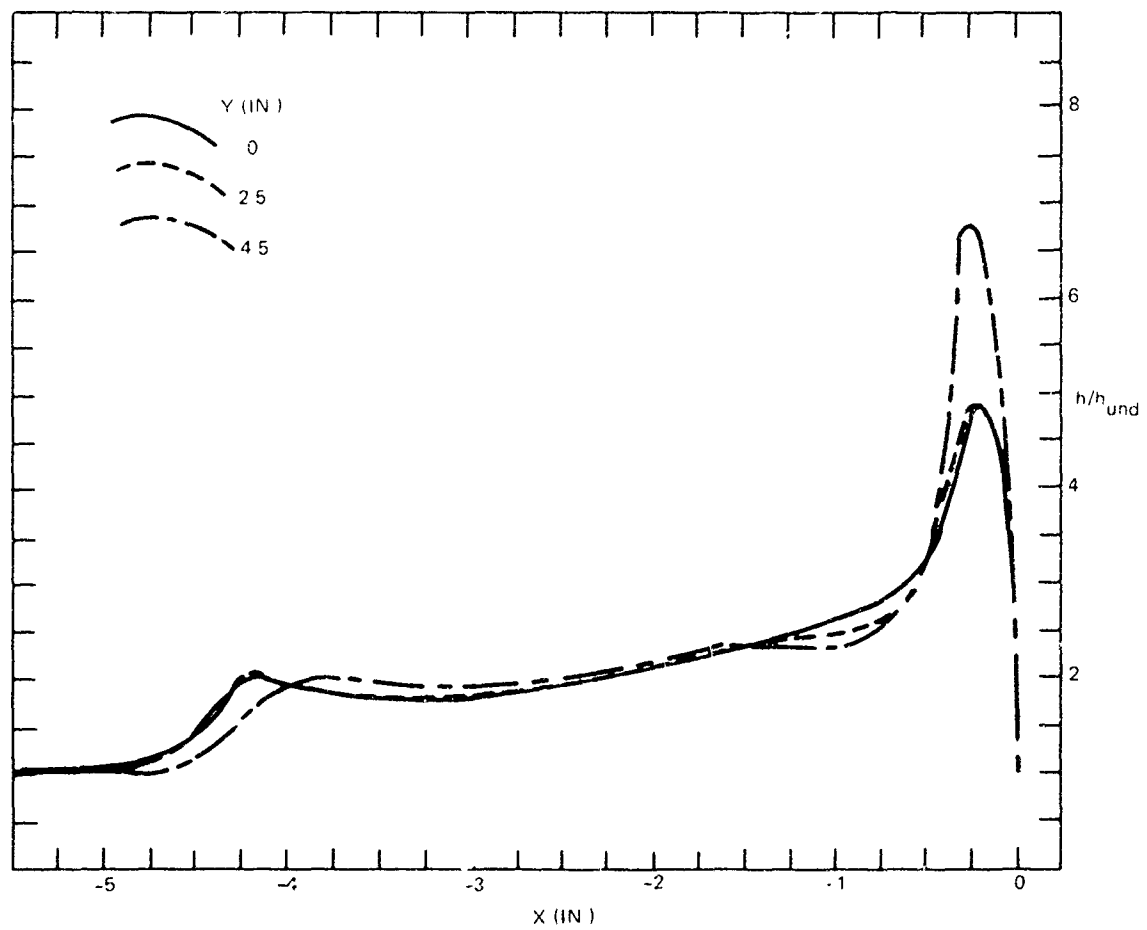
Figure 42   Streamwise Distributions of Heat Transfer Coefficient Ratios on Plate Surface for M_1 = 4.75 Flow Ahead of 10-inch Span Step
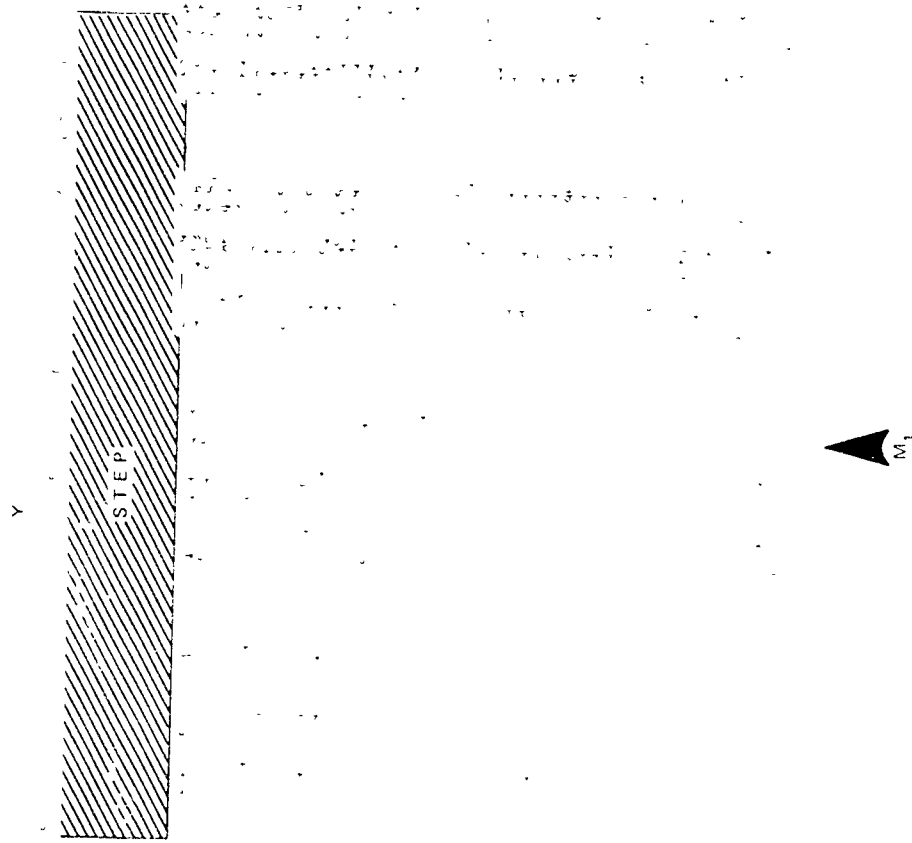
Figure 43   Frame from Motion Picture Showing ... Surface ... Spin Step for M_3 ... 4.75
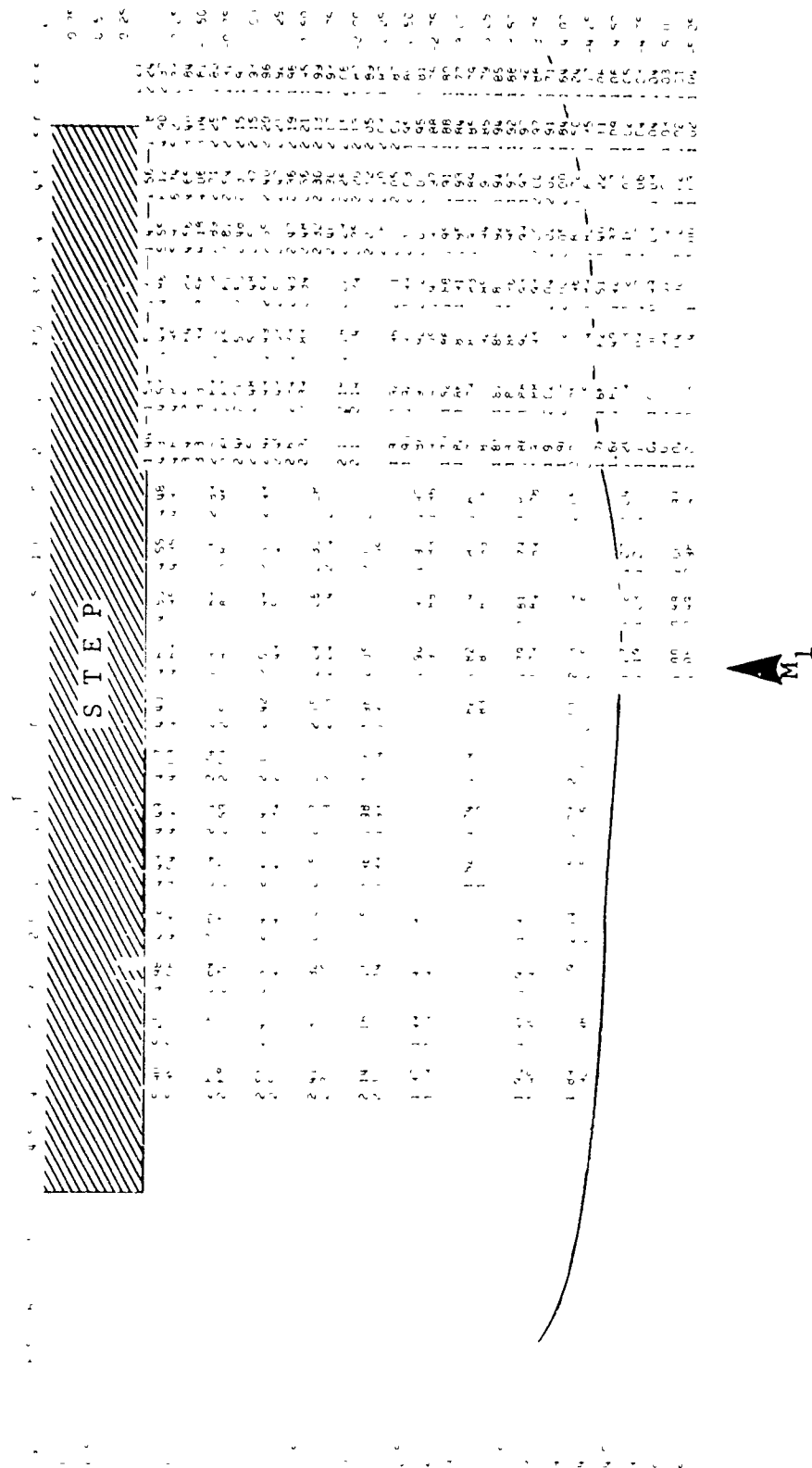
Figure 44   Distribution of Heat Transfer Coefficient Ratios (h/h_{und}) on Surface Ahead of 10-inch Span Step for M_1 = 4.75
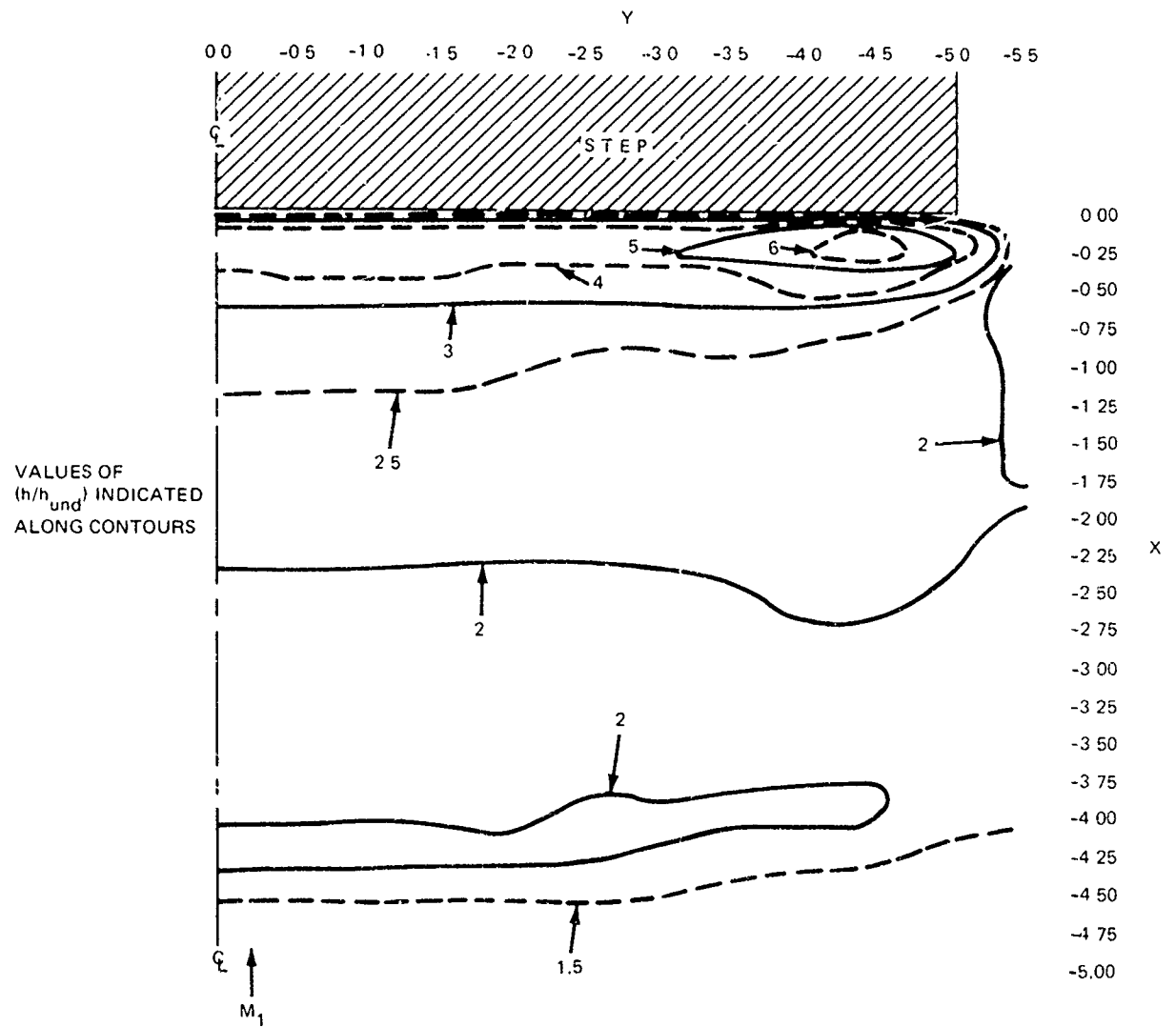
Figure 45   Lines of Constant (h/h_{und}) Contours on Surface Ahead of 10-inch Span Step for M_1 = 4.75

55
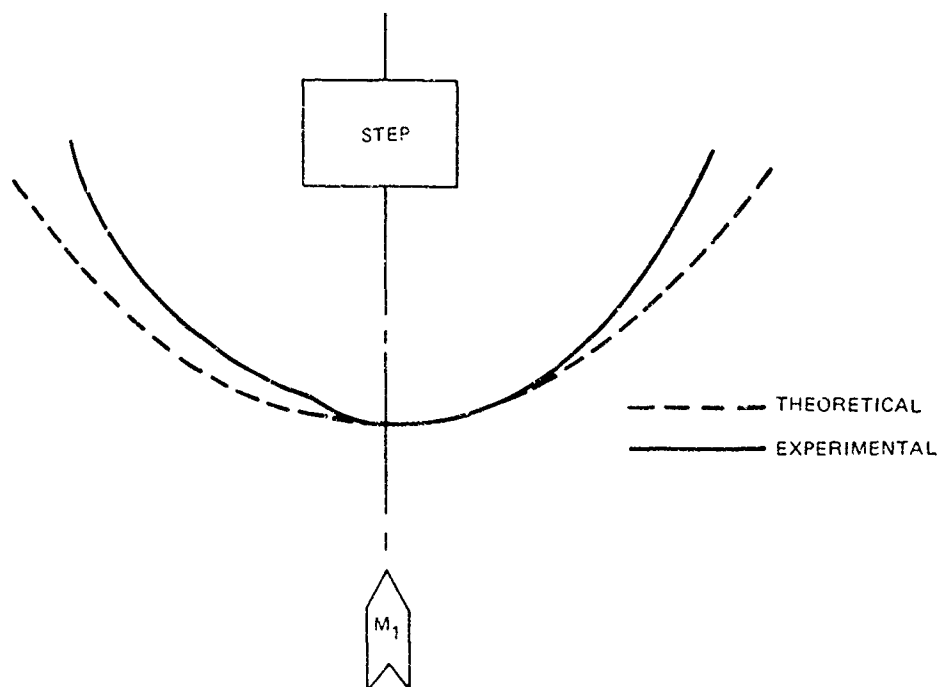
Figure 46   Comparison of Predicted and Experimental Separation Lines on Surface Ahead of 3-inch Span Step for M_1 = 5.04

Figure 47 Comparison of Predicted and Experimental Separation Lines on Surface Ahead of 5-inch Span Step for $M_1 = 5.04$

Figure 48   Comparison of Predicted and Experimental Separation Lines on Surface Ahead of 7-inch Span Step for M_1 = 5.04

STEP

b = 10″

M₁

— — — THEORETICAL
————— EXPERIMENTAL
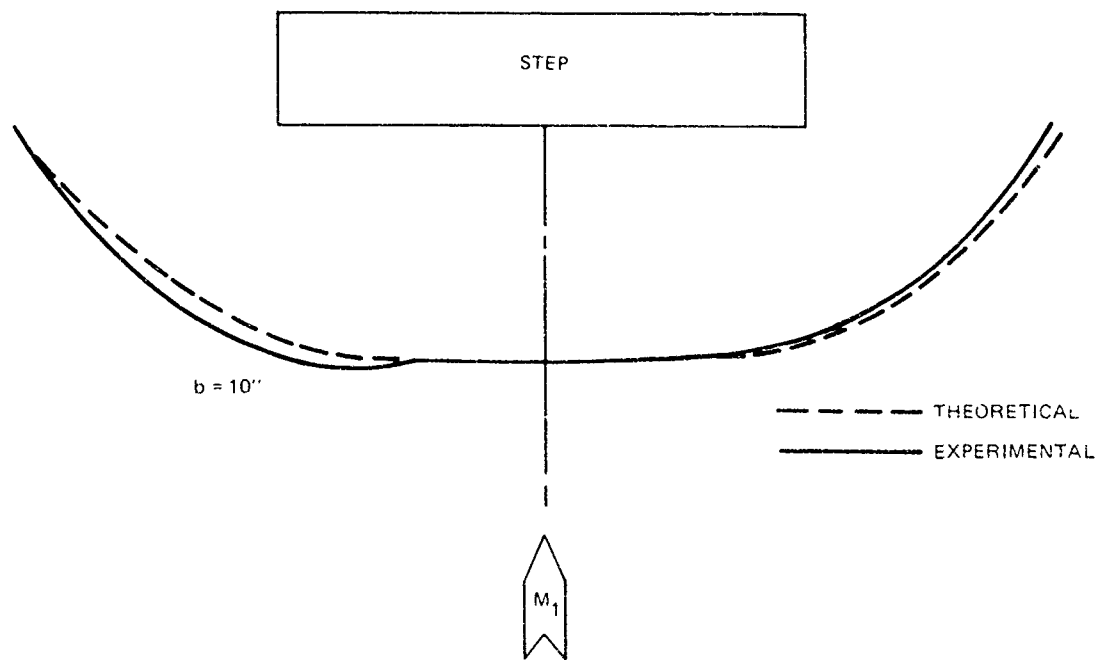
Figure 49   Comparison of Predicted and Experimental Separation Lines on Surface Ahead of 10-inch Span Step
for M_1 = 5.04

REFERENCES

1. Law, C. H., "Supersonic Shock Wave Turbulent Boundary Layer Interactions," AIAA J., Vol. 14, No. 6, June 1976.

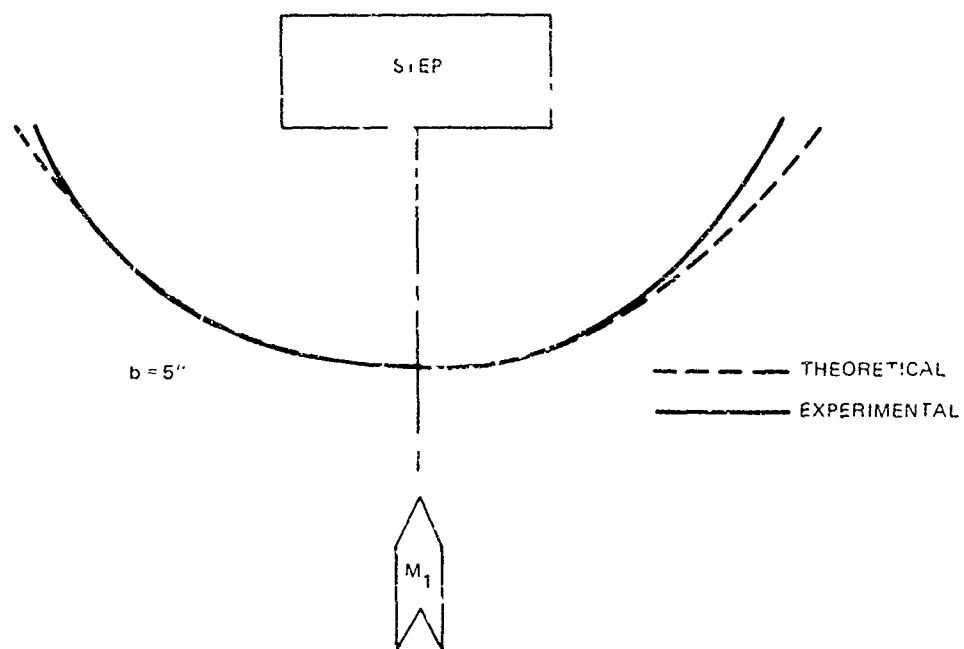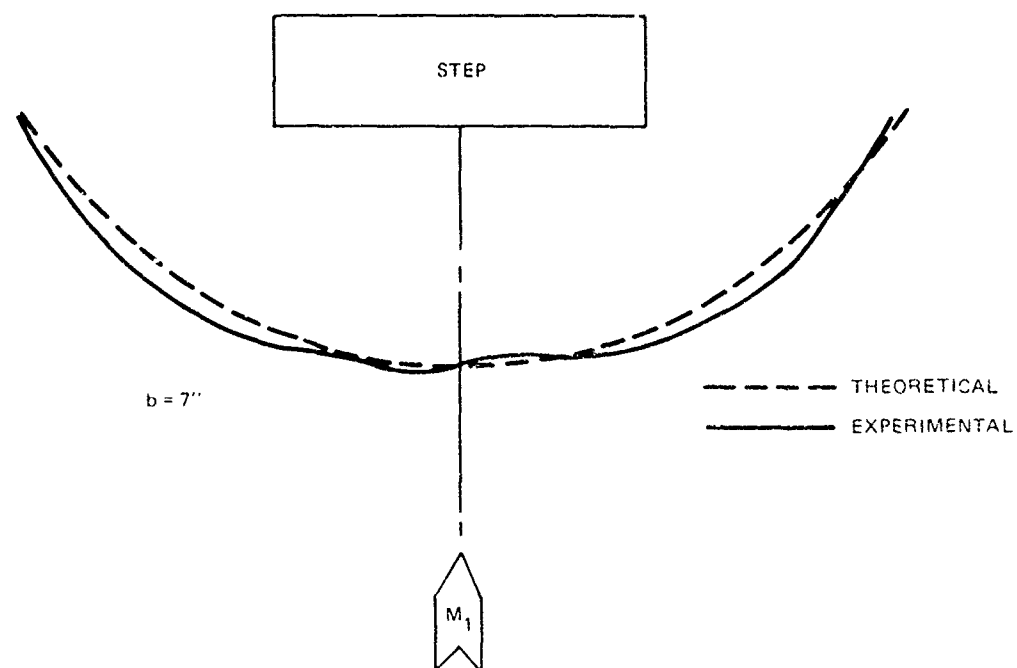2. Settles, G. S., Bogdonoff, S. M., and Vas, I. E., "Incipient Separation of a Supersonic Turbulent Boundary Layer at High Reynolds Numbers," AIAA J., Vol. 14, No. 1, January 1976.

3. Korkegi, R. H., "On the Structure of Three Dimensional Shock Induced Separated Flow Regions," AIAA Paper 76-165, January 1976.

4. Sedney, R. and Kitchens, C. W. Jr., "Measurement and Correlation of Separation Ahead of Protuberances in a Turbulent Boundary Layer," AIAA Paper 76-163, January 1976.

5. Schepers, H. J., "Untersuchungen der wandnahen stroemung und des Waermeuebergangs im Bereich langsangestroemter Ecken bei Hyperschallanstroemung," Deutsche Luft-und Raumfahrt, DLR-FB 76-02, 1976.

6. Czarnecki, K. R. and Jackson, M. W., "Turbulent Boundary Layer Separation Due to a Forward-Facing Step," AIAA J., Vol. 13, No. 12, December 1975.

7. Rao, D. M., "Hypersonic Incipient Separation on Delta Wing with Trailing Edge Flap," AIAA J., Vol. 13, No. 10, October 1975.

8. Korkegi, R. H., "Viscous Flow Interaction Studies," Aerospace Research Laboratories TR 75-0164, AD # A015191, Wright-Patterson AFB, July 1975.

9. Christophel, R. G., "Two Dimensional Shock Wave Boundary Layer Interactions," AFFDL TR 74-152, AD#A016469, Wright-Patterson AFB, July 1975.

10. Bogdonoff, S. M., Vas, I. E., Settles, G. S., and Simpers, G., "Research on Supersonic Turbulent Separated and Re-attached Flows," Aerospace Research Laboratories Report 75-0220, AD#A014769, Wright-Patterson AFB, June 1975.

11. Kaufman, L. G. II and Freeman, L. M., "Separation Ahead of Controls on Swept Wings," Aerospace Research Laboratories TR 75-0134, AD#A014240, Wright-Patterson AFB, June 1975.

12. Sedney, R. and Kitchens, C. W. Jr., "The Structure of Three Dimensional Separated Flows in Obstacle, Boundary Layer Interactions," AGARD Conference on Flow Separation, AGARD CPP 168, May 1975.

13. Korkegi, R. H., "Comparison of Shock-Induced Two and Three Dimensional Incipient Turbulent Separation," AIAA J., Vol. 13, No. 4, April 1975.

14. Oskam, B., Bogdonoff, S. M., and Vas, I. E., "Study of Three Dimensional Flow Fields Generated by the Interaction of a Skewed Shock Wave with a Turbulent Boundary Layer," AFFDL TR 75-21, AD#A014837, Wright-Patterson AFB, February 1975.

15. Law, C. H., "Supersonic, Turbulent Boundary Layer Separation," AIAA J., Vol. 12, No. 6, June 1974.

16. Token, K. H., "Heat Transfer Due to Shock Wave Turbulent Boundary Layer Interactions on High Speed Weapon Systems," AFFDL TR 74-77, AD#A002685, Wright-Patterson AFB, April 1974.

17. Driftmyer, R. T., "Thick, Two Dimensional, Turbulent Boundary Layers Separated by Steps and Slot Jets," AIAA J., Vol. 12, No. 1, January 1974.

18. Coleman, G. T. and Stollery, J. L., "Incipient Separation of Axially Symmetric Hypersonic Turbulent Boundary Layers," AIAA J., Vol. 12, No. 1, January 1974.

19. Goldberg, T. J., "Three Dimensional Separation for Interaction of Shock Waves with Turbulent Boundary Layer," AIAA J., Vol. 11, No. 11, November 1973.

20. Reda, D. C. and Murphy, J. D., "Shock Wave/Turbulent Boundary Layer Interactions in Rectangular Channels," AIAA J., Vol. 11, No. 2, February 1973.

21. Peake, D. J., Rainbird, W. J., and Atraghji, E. G., "Three Dimensional Flow Separations on Aircraft and Missiles," AIAA J., Vol. 10, No. 5, May 1972.

22. Whitehead, A. H. Jr., Sterrett, J. R., and Emery, J. C., "Effects of Transverse Outflow from a Hypersonic Separated Region," AIAA J., Vol. 10, No. 4, April 1972.

23. Haslett, R. A., Kaufman, L. G. II, Romanowski, R. F., and Urkowitz, M., "Interference Heating Due to Shock Impingement," AFFDL TR-72-66, AD#749946, Wright-Patterson AFB, July 1972.

24. Neumann, R. D., "Recent Notes and Data on Interference Heating," AFFDL TR 72-12, AD#747765, Wright-Patterson AFB, May 1972.

25. Ball, K. O. W., "Flap Span Effects on Boundary Layer Separation," AIAA J., Vol. 9, No. 10, October 1971.

26. Korkegi, R. H., "Survey of Viscous Interactions Associated with High Mach Number Flight," AIAA J., Vol. 9, No. 5, May 1971.

27. Murphy, J. D., "A Critical Evaluation of Analytic Methods for Predicting Laminar Boundary Layer, Shock Wave Interaction," NASA TN D-7044, January 1971.

28. Hill, W. G. Jr., "A Comparison of Theory and Experiment for Laminar Separation Ahead of a Compression Corner at Supersonic and Low Hypersonic Speeds, Grumman Research Department Report RE-401, December 1970.

29. Johnson, C. B., "Heat Transfer Measurements at Mach 8 on a Flat Plate with Deflected Trailing Edge Flap with Effects of Transition Included," NASA TN D-5899, July 1970.

30. Ryan, B. M., "Summary of Aerothermodynamic Interference Literature," Naval Weapons Center (China Lake, California), TN 4061-160, April 1969.

31. Neumann, R. D. and Burke, G. L., "The Influence of Shock Wave Boundary Layer Effects on the Design of Hypersonic Aircraft," AFFDL TR 68-152, AD#686738, Wright-Patterson AFB, March 1969.

32. Whitehead, A. H. Jr. and Keyes, J. W., "Flow Phenomena and Separation Over Delta Wings with Trailing Edge Flaps at Mach 6," AIAA J., Vol. 6, No. 12, December 1968.

33. Keyes, J. W., Goldberg, T. J., and Emery, J. C., "Turbulent Heat Transfer Associated with Control Surfaces at Mach 6," AIAA J., Vol. 6, No. 8, August 1968.

34. Johnson, C. B., "Pressure and Flow Field Study at Mach Number 8 of Flow Separation on a Flat Plate with Deflected Trailing Edge Flap," NASA TN D-4308, March 1968.

35. Zukoski, E. E., "Turbulent Boundary Layer Separation in Front of a Forward Facing Step," *AIAA J.*, Vol. 5, No. 10, October 1967.

36. Zukoski, E. E., "Review of Data Concerning Turbulent Boundary Layer Separation in Front of a Forward Facing Step," Guggenheim Jet Propulsion Center, C.I.T., Report 66-8-15-1, August 1966.

37. McCabe, A., "The Three Di ensional Interaction of a Shock with a Turbulent Boundary Layer," *The Aeronautical Quarterly*, pp. 231-252, August 1966.

38. Chapman, D. R., Kuehn, D. M., and Larson, H. K., "Investigation of Separated Flows in Supersonic and Subsonic Streams with Emphasis on the Effect of Transition," NACA Report 1356, 1958.

39. Holloway, P. F., Sterrett, J. R., and Creekmore, H. S., "An Investigation of Heat Transfer within Regions of Separated Flow at a Mach Number of 6.0," NASA TN D-3074, November 1965.

40. Sterrett, J. R. and Emery, J. C., "Extension of Boundary Layer Separation Criteria to a Mach Number of 6.5 by Utilizing Flat Plates with Forward Facing Steps," NASA TN D-618, 1960.

41. AEDC Staff, "von Karman Gas Dynamics Facility," *Test Facilities Handbook* (10th Edition), Arnold Engineering Development Center, May 1974.

42. Anderson, E. C. and Lewis, C. H., "Laminar or Turbulent Boundary Layer Flows of Perfect Gases or Reacting Gas Mixtures in Chemical Equilibrium," NASA CR 1893, 1971.

43. Ames Research Staff, "Equations, Tables, and Charts for Compressible Flow," NACA Report 1135, 1953.

44. Liepmann, H. W. and Roshko, A., "Elements of Gas Dynamics," John Wiley & Sons, Inc., New York, p. 87, 1957.